GEOTECHNICAL RESEARCH CENTRE

CONTAMINANT TRANSPORT AND ENVIRONMENTAL ENGINEERING

by

Raymond N. Yong and GRC Staff

SOIL MECHANICS SERIES No. 56

July 1990

McGill University
Montreal, Que Canada

ISSN 0541-6329

FOREWORD

The following selection of papers on CONTAMINANT TRANSPORT AND ENVIRONMENTAL ENGINEERING has recently been published in the Proceedings of the 1990 Canadian Society for Civil Engineering (CSCE) Annual Conference on ENGINEERING IN OUR ENVIRONMENT, held in Hamilton, Ontario - May 1990.

1. Yong, R.N.
   "Contaminant Transport: Physical and Analytical Modelling Requirements and Problems"

2. Yong, R.N., Mohamed, A.M.O. and Samani, H.M.
   "Adsorption/Desorption in Multi-Component Contaminant Transport in Clay Barriers"

3. Yong, R.N. and Chen, C.K.
   "Self Sealing of Aerated Stabilization Basin for Bleached Kraft Wastewater Sludges"

4. Yong, R.N. and Warith, M.A.
   "Groundwater Contamination by Industrial and Domestic Wastes"

CONTAMINANT TRANSPORT: PHYSICAL AND ANALYTICAL MODELLING REQUIREMENTS AND PROBLEMS

RAYMOND N. YONG[1]

EXTENDED ABSTRACT

In this *THEME* presentation on the problems which need to be considered in modelling contaminant transport through clay soils, the central focus of the discussion is on clay-contaminant interaction and fate, in relation to specification of the transport coefficient D and accountability for adsorption and desorption reactions. Most of the models in common practice are Fickian in nature and generally consist of a set of equations which describe the physical/chemical process being studied. Questions with respect to *how well - i.e. how accurately - is the physical/chemical problem characterized?* are fundamental to the thesis which insists that the physical/chemical problem must be properly mimicked (by the analytical model).

The general procedure for development of the sets of differential equations describing contaminant transport in soils combines the equation of motion (flow equation for the water) with the convective-dispersion equation for mass transport of the contaminants. This is by and large, the mass transport model which considers both quantity and quality of the groundwater flow. Whether (or not) the various models consider the many processes that influence mass transport, and how well these models properly reflect the relationships described by these processes, constitute the issues at hand. It is recalled that the various processes that control mass transport can be grouped into three principal categories:

---

[1] **William Scott Professor of Civil Engineering and Applied Mechanics, Director, Geotechnical Research Centre, McGill University, Montreal.**

- ** PHYSICAL
  - advection, hydrodynamic dispersion, molecular diffusion, and density stratification;
- ** PHYSICO-CHEMICAL AND CHEMICAL
  - mechanisms of accumulation (physisorption, chemisorption, complexation, desorption, speciation, precipitation, etc.), oxidation-reduction reactions, immiscible phase partitioning;
- ** BIOLOGICAL
  - biotransformation, co-metabolism, biotransformation and microbial population dynamics;

We can consider transport in (a) the unsaturated zone, (b) the unsaturated zone and into the saturated zone, and/or (c) the saturated zone. The development of the relationships for transport in the saturated zone, in terms of Fickian relationships or irreversible thermodynamics, has been well covered by many researchers, e.g. Ogata, (1970), Frind (1987), Konokow and Grove, (1977), Rowe, (1987), Yong and Samani (1987), Taylor and Cary, (1964). A sample of the various equations, written to represent the one-dimensional case (for simplicity) is given as follows:

$$\frac{\partial c}{\partial t} + v_x \frac{\partial c}{\partial x} = D \frac{\partial^2 c}{\partial x^2} \tag{1}$$

$$\frac{\partial c}{\partial t} + v_x \frac{\partial c}{\partial x} = D \frac{\partial^2 c}{\partial x^2} \pm \frac{\rho_s}{n} \frac{\partial S}{\partial t} \tag{2}$$

where:

c = concentration of particular contaminant species being considered,
v_x = average advective velocity,
ρ_s = dry density of soil
n = porosity of soil
S = mass of particular contaminant species adsorbed per unit mass of dry soil,
x, t = spatial and time variables
D = "diffusion-dispersion" coefficient.

Equation (1) is the familiar "diffusion/dispersion"-advection relationship, and equation (2) represents the adsorption-desorption "add-on" to equation (1) – via the last term on the RHS in equation (2). The points of interest are (a) the coefficient D, and (b) the adsorption relationship S. The adsorption phenomenon can also be handled via a retardation factor R, as for example the kind of relationship used by Hashimoto et al (1964), Davidson and Chang (1972):

$$D \frac{\partial^2 c}{\partial x^2} - \frac{v_x}{R} \frac{\partial c}{\partial x} = R \frac{\partial c}{\partial t} \tag{3}$$

In this case, the retardation factor R is given as:

$R = 1 + \frac{\rho_b}{\theta} K_d$
ρ_b = bulk density of the saturated soil,
θ = effective porosity, (volumetric water content),

K_d = distribution coefficient governing partitioning of particular contaminant species into dissolved and adsorbed phases – akin to the philosophy governing the use of the adsorption isotherm in equation (2).

The coefficient D is difficult to fully identify or quantity. Whilst some researchers have used different terms to identify D, the concensus terminology appears to center around the one used herein, i.e. "diffusion-dispersion" coefficient. The use the seemingly awkward terminology reflects not only the difficulties in proper assesment of the mechanisms controlling attenuation of the various contaminant component species, but also the manner in which these mechanisms should be "modelled".

Modelling of the fate of the particular contaminant species via evaluation of adsorption or desorption mechanisms (and isotherms), or via the use of linear or non-linear partitioning functions is also of considerable concern. Both D and S or R pay attention to a particular solute (contaminant species) at any one time. Thus, for a spate of contaminant consitutuents, it is necessary to perform the computational exercise separately for each constituent species. However, if one recognizes that the behaviour and fate of each constituent species depends on the concentrations and types of the other constituents (i.e. concentrations and distributions), then it becomes clear that extrapolation of any of the coefficients or relationships for general "field" application must pay particular attention to how well the field leachate contaminant is mimicked – in composition variation (constituent concentration and distribution) with time and space!

The common procedures for modelling generally discount, ignore or perhaps simply forget about chemico-osmotic flow. To determine whether this oversight is particularly significant (or not), one needs to be reminded that determination of the D coefficient is often performed using measurement of chemical fluxes across the domain of interest, and application of the Fickian model for "back calculation" of the D coefficient. In situations where advective flow is negligible, this chemico-osmotic flow term could be a significant factor influencing measured values of transport – *viz* calculations of the D coefficient based on flux measurements could be in serious error. It is apparent that in the face of these various "forces", modelling of the transport of any particular species of contaminant constituent becomes very challenging.

BIBLIOGRAPHY

Ogata, A., (1970) "Theory of Dispersion in a Granular Medium" U.S. Geological Survey Paper, 411-I

Frind, E. O., (1987) "Modelling of Contaminant Transport in Groundwater: An Overview" Proc. CSCE Centennial Symposium on Management of Waste Contamination of Groundwater, Montreal, pp. 1-30

Konokow, L. F., and Grove, D. B., (1977) "Derivation of Equations Describing Solute Transport in Groundwater", U.S. Geological Survey, Water Resources Investigation, No. 77-19

Rowe, K., (1987) "Pollutant Transport Through Barriers", Proc. Geotechnical Practice for Waste Disposal, ASCE, pp 159-181

Taylor, S. A., and Cary, J. W., (1964) "Linear Equations for the Simultaneous Flow of Matter and Energy in a Continuous Soil System", Soil Sci. Soc. Amer. Proc. 28: 167-172

Yong, R., N., and Samani, H. M. V., "Modelling of Contaminant Transport in Clays Via Irreversible Thermodynamics", Proc. Geotechnical Practice for Waste Disposal, ASCE, pp.846-860

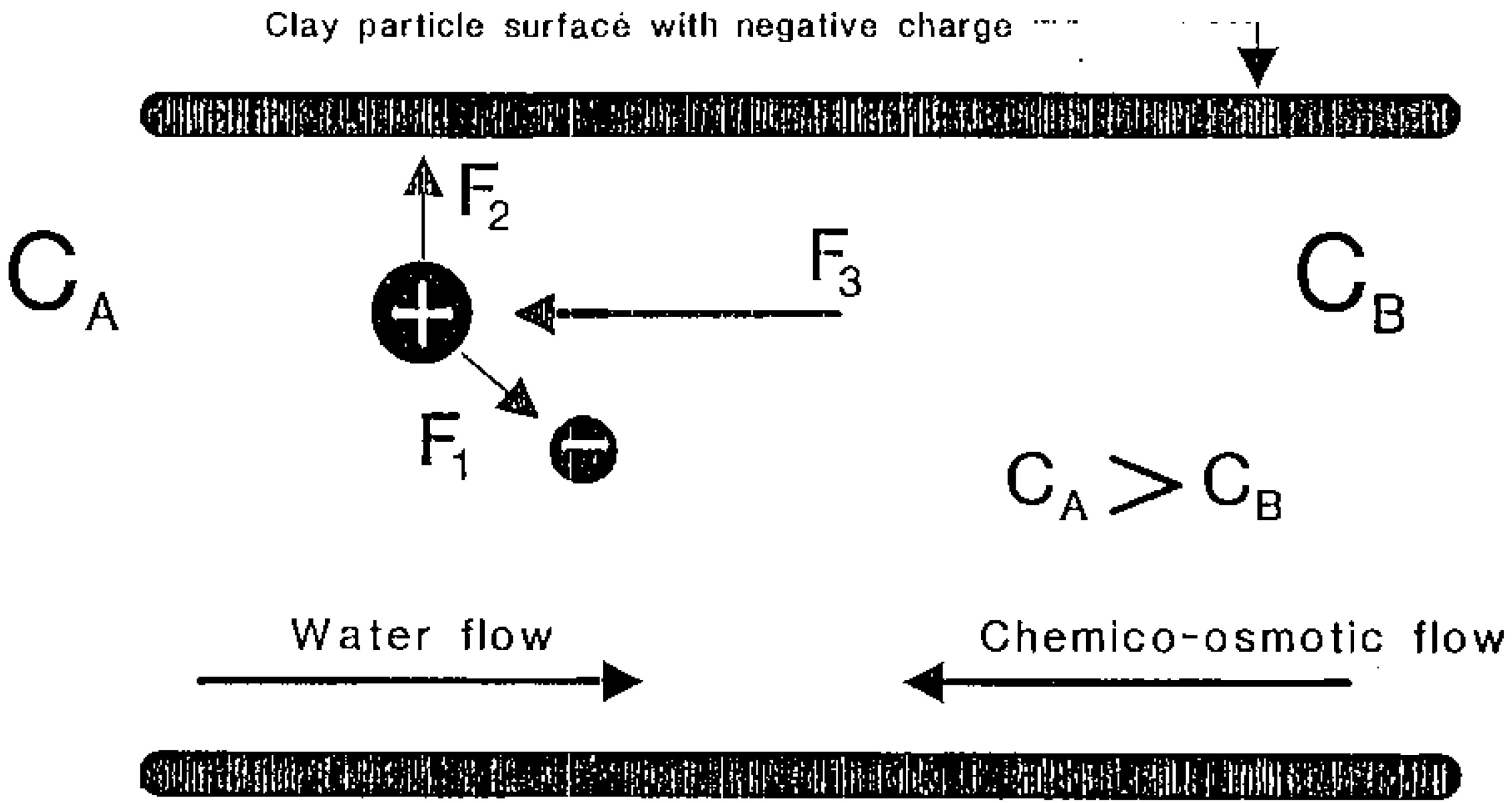

Fig. 1 - Pollutant cation diffusion-interaction with clay

(F_3 is resistance force of fluid)

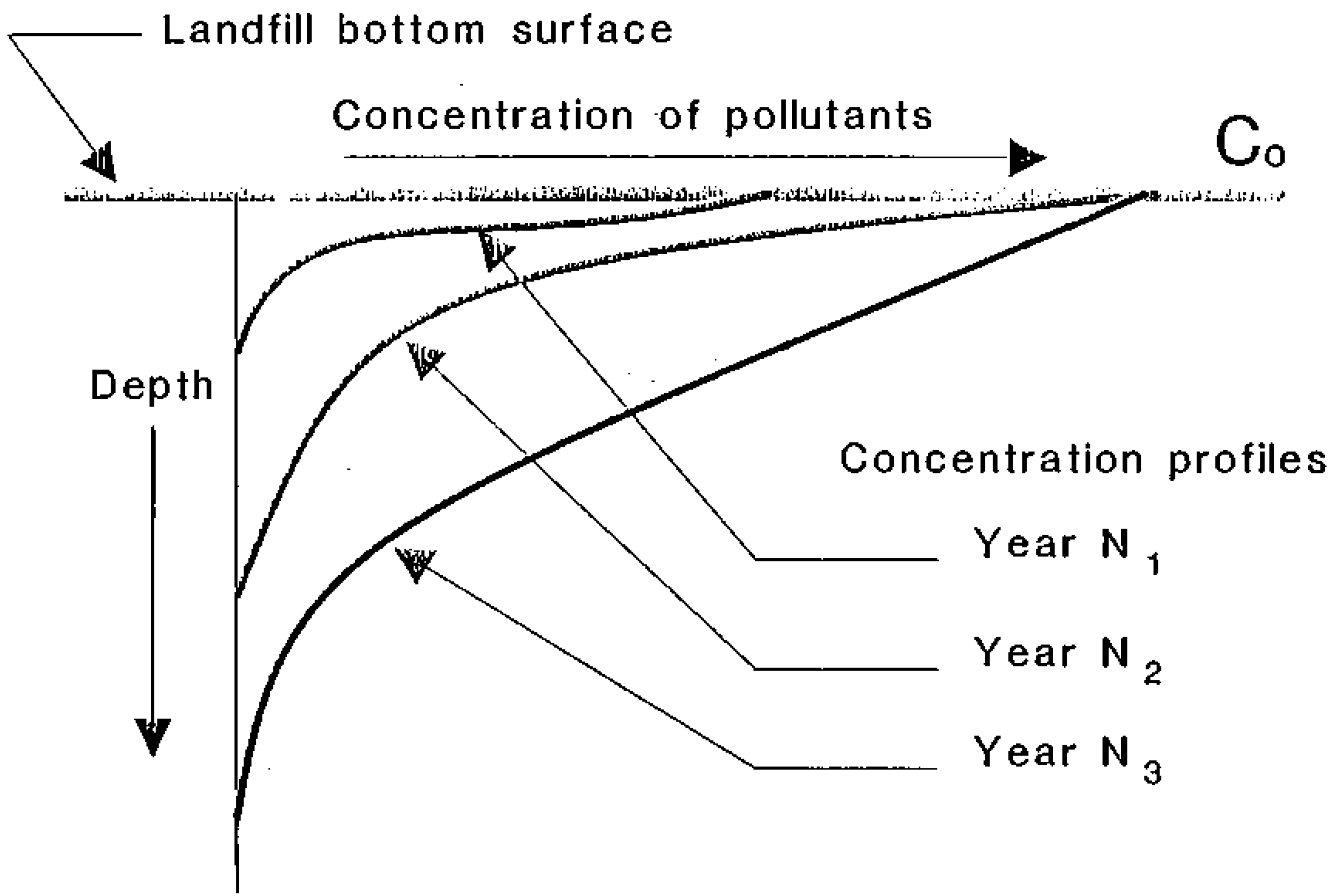

Fig. 2 - Diffusion profiles

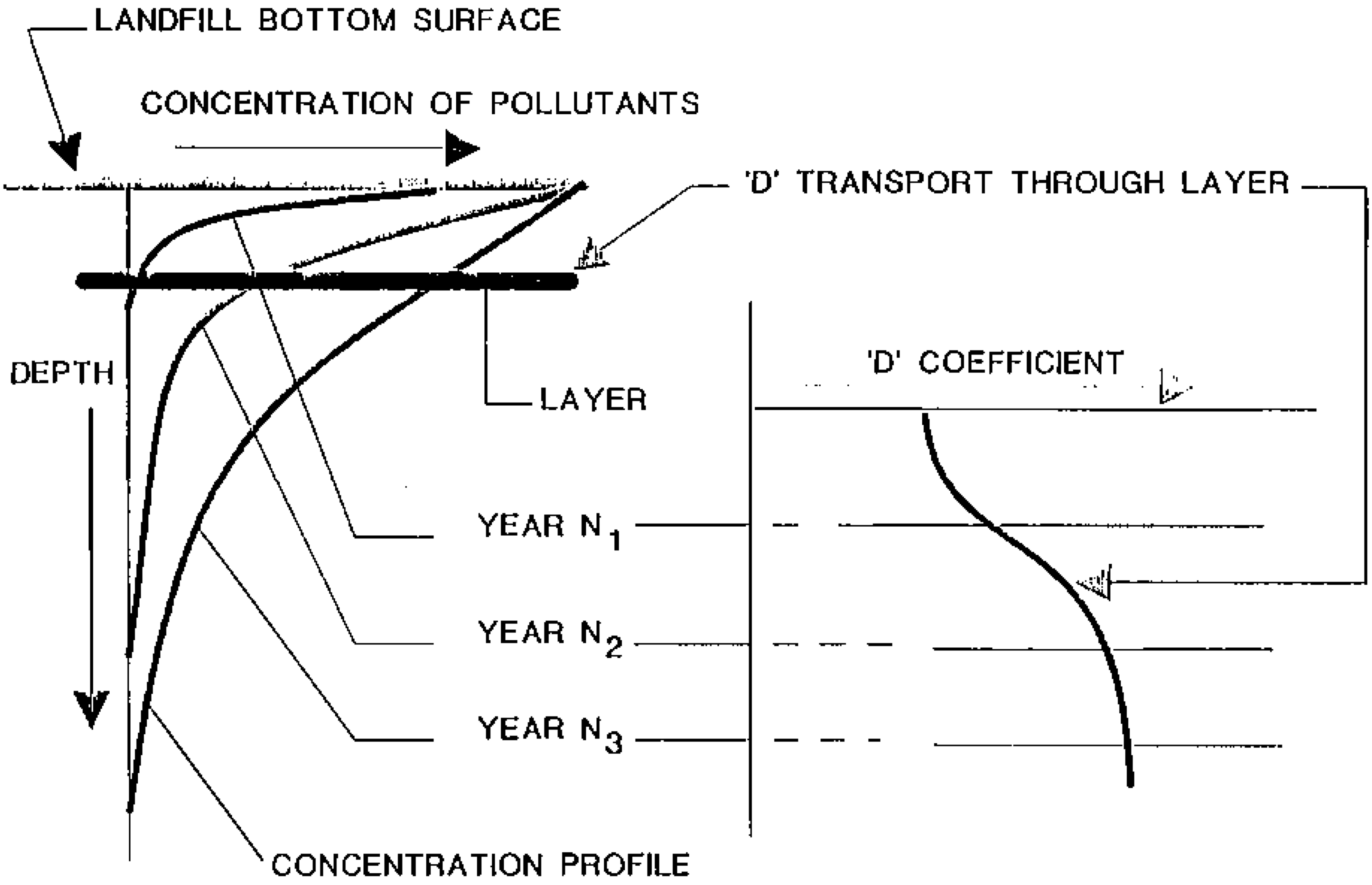

Fig. 3 - 'D' Coefficient variation with time

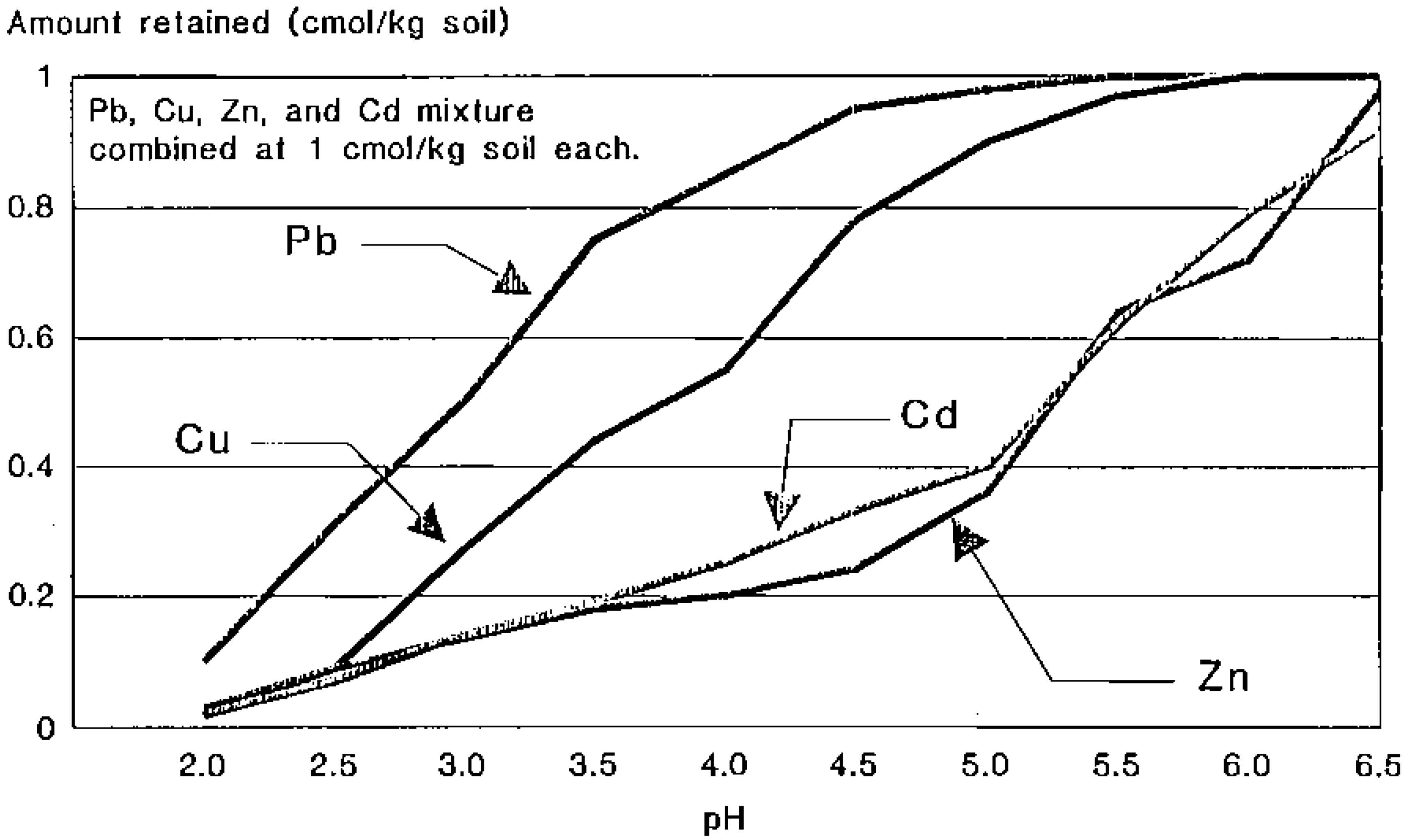

Fig 4 - Heavy metal retention in a natural clay

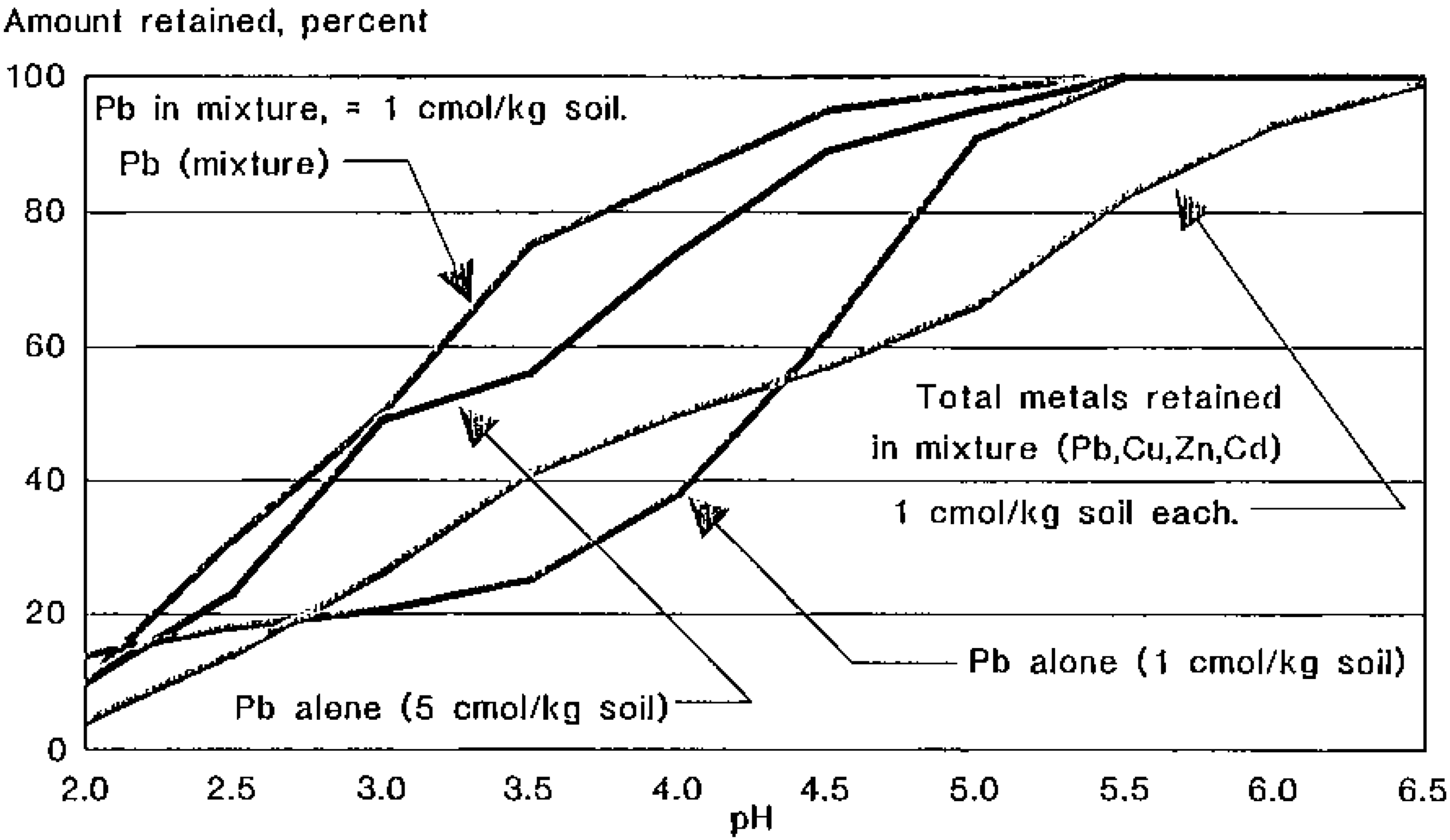

Fig. 5 - Pb retention in a natural clay soil

(Pb alone in mixture, mixture, & alone)

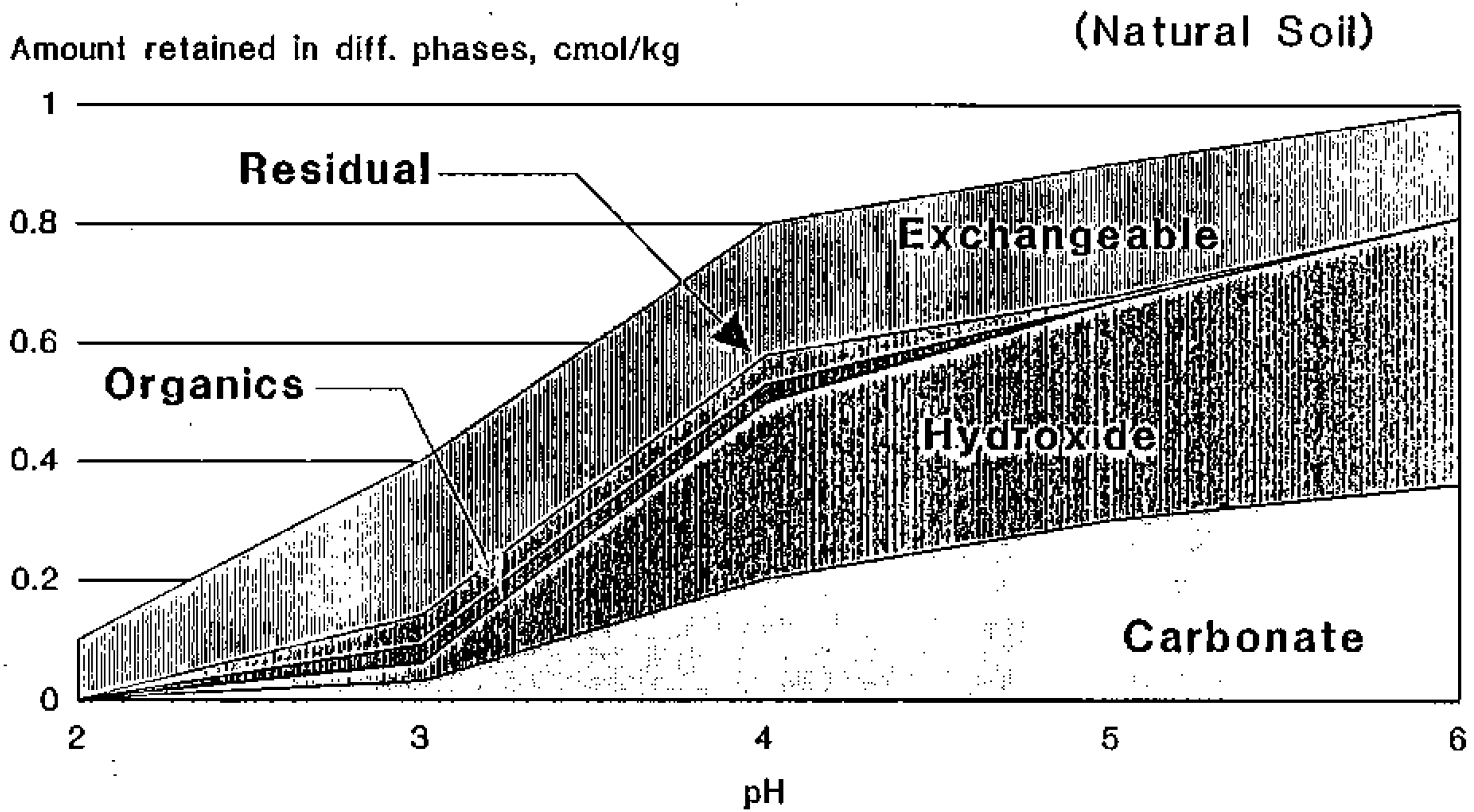

Fig. 6 - Pb retention in different phases, cmol/kg soil

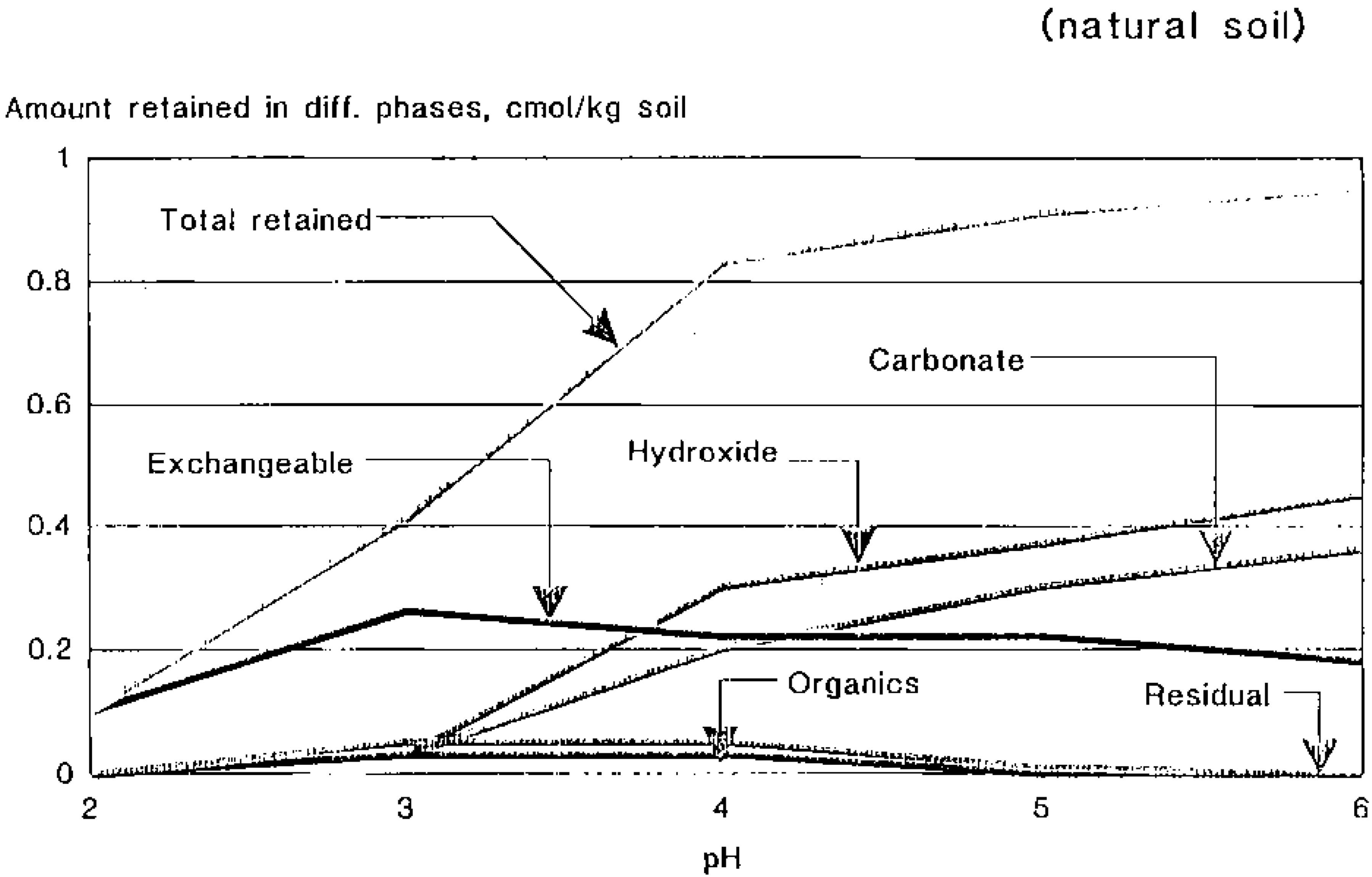

Fig. 7 - Pb retention in different phases

ADSORPTION/DESORPTION IN MULTI-COMPONENT CONTAMINANT TRANSPORT IN CLAY BARRIERS

R. N. Yong,[1] A. M. O. Mohamed,[2] and H. M. Samani[3]

ABSTRACT

This study develops a multi-component adsorption/desorption model using input from laboratory measurents. Accountability for adsorption and desorption processes in contaminant transport is obtained from laboratory experimental leaching tests with different types of soils and a multi-component contaminant leachate obtained from a landfill site. The measurements made include analysis of influent, effluent, and retained contaminant species (and concentrations with time). In the multi-component adsorption/desorption model developed from the experimental results obtained, the five parameters used in the model account for the various types of solute contaminant components and soil systems. These parameters are estimated by using Powell's method in nonlinear optimization of experimental results obtained from laboratory leaching cell tests. The developed model is applied to an operating field land disposal site to predict contaminant transport performance over a period of a few hundred years.

---

[1] William Scott Professor of Civil Engineering and Applied Mechanics, Director, Geotechnical Research Centre, McGill University, Montreal.

[2] Research Associate, Geotechnical Research Centre, McGill University, Montreal.

[3] Chairman, Department of Civil Engineering, Ahwaz University, Iran.

INTRODUCTION

Adsorption/desorption of ions occur as a result of clay-contaminant interaction in clay soils, and thus need to be considered in clay barrier design for buffering of contaminant transport. Adsorption is defined as the transfer of solute ions from the pore fluid solution to the solid phase, whereas desorption is defined as the reversible interchange of ions between the colloid particle surfaces and the solution. The impact of adsorption/desorption in the clay soil barriers becomes particularly important in the context of the various considerations or recommendations set forward by the regulatory bodies (in Canada) concerning, e.g. *Reasonable Use Policy*, land disposal of wastes. The implicit reqiurement for **attenuation** of contaminant transport carries with it a higher requirement for understanding of the various issues of clay-contaminant interaction which are needed to *support the attenuation requirement*.

Changes in the composition, availability, and amount of leachate migrating from waste containment ponds and landfills for industrial and domestic wastes result directly from rainfall frequency and infiltration (seepage), and reaction kinetics established within the waste mass between the solids and influent liquid. The manner in which the generated leachate is contained, buffered, and transported through the soil barrier is a function of (1) the controlling mechanisms of transport through the soil buffer system – e.g. diffusive or dispersive mass transport; and (2) the interactions and reactions that occur between contaminant leachate and soil system – e.g. adsorption of contaminants onto surfaces of soil constituents; ion-exchange; microbial interaction and activity leading to biodegradation and generation of various products; and precipitation. Depending on the nature and composition of the contaminant leachate, these processes may be of varying importance and significance in the control of leachate migration through clay soil barriers. In the reaction processes resulting from contaminant-soil interaction, it is acknowledged that desorption also occurs, thereby resulting in changes in the composition and concentration of the various ion species in the leachate. In this process, some of the leachate components will be adsorbed on clay particle surfaces while others (initial cations or other previously adsorbed contaminant ions) will be desorbed due to ion exchange. Hence, to model the desorption of a certain component ionic species, information about the behavior and migration of other species is required, i.e. the transport of all solute components involved in the problem has to be determined simultaneously. The need for modeling of adsorption-desorption is thus considered to be an important element in the evaluation and analysis of contaminant transport in the soil barrier or substrate.

In this study, ion desorption in a clay barrier material is evaluated through the use of leaching cell experiments, and a multi-component adsorption desorption model. By using the actual leachate from an operating landfill site, previously described by Yong et al. (1987), model calibration is obtained from the leaching experiments, and predictions can be made for migration of the various contaminant ions in the landfill.

Adsorption and Desorption

Since a significant portion of the accumulation process for attenuation of contaminant transport relies on adsorption mechanisms, it is useful to recall the various factors that affect adsorption of a contaminant species onto a soil surface. These include (Stumm and Morgan, 1970; Weber, 1975; Yong et al, 1990;):

1) soil specific surface area;
2) concentration and nature of the adsorbate (contaminants);
3) initial soil and contaminant pH;
4) temperature;
5) concentration;
6) nature and distribution of the competing ions present in the intruding solution (leachate solution);
7) the nature of the adsorbent (soil system).

Whilst it is expedient to categorize adsorption mechanisms in terms of:

(a) physical adsorption - involving only relatively weak intermolecular forces;

(b) chemisorption – which essentially involves formation of a chemical bond between the sorbate molecule and the surface of the adsorbent,

there exist many intermediate cases which do not make it possible to categorize unequivocally. The general features which distinguish physical adsorption from chemisorption, presented in Table 1, demonstrate the problem.

The forces involved in physical adsorption include both van der Waals forces and electrostatic interactions comprising polarization, dipole, and quadrupole interactions. The van der Waals contribution is always present whereas the electrostatic contributions are significant only in the case of adsorbents which have ionic structures. However, for the sorption of small dipolar molecules such as water, electrostatic contribution may be very large, giving rise to measurable heats of adsorption. Thus, although such interactions are properly regarded as physical adsorption, the heat of adsorption may well be of a magnitude generally associated with chemisorption. Furthermore, in such systems the adsorption is quite specific and the rate is often controlled by an activated diffusion process, giving the appearance of a slow activated chemisorption, even though the actual surface adsorption may be rapid. Thus such systems may appear to exhibit many of the characteristic factors generally associated with chemisorption.

Of the several equilibrium and non-equilibrium adsorption models which exist, the most popular are the Langmuir and Freundlich models. It should be noted that all models are designed to portray the adsortion relationship between a particular contaminant species (absorbate) and the soil system (absorbent). The correct modeling of an absorbate undergoing both transport and adsorption through a clay soil system necessitates the selection of an adsorption model that best suits the given system. The use of an improper adsorption model will greatly affect the transport model, and will possibly give rise to erroneous conclusions regarding the nature and description of both parameters and processes of the system analyzed. In that regard, it is particularly useful to obtain similar conditions of absorbate-absorbent interactions for specific model application if one chooses to model adsorption for a chosen problem. To do so, it is necessary to obtain matching of both absorbate and absorbent compositions. Thus for example, the linear equilibrium isotherm adsorption relationship which states that the rate of adsorption is constant may not be physically valid, since the ability of clay particles to adsorb solute ions decreases as the adsorbed amount of that solute ions increases. Similarly, if the rate of adsorption decreases rapidly as the concentration in the pore fluid increases, the simple Freundlich type models will need to be extended to properly portray the adsorption relationship developed.

Since very few (if any) can faithfully portay the adsorption relationship for multi-component leachate systems where some of the components are adsorbed and some others are desorbed, it is necessary to perform one's own tests with the "real system" to obtain the adsorption model specific to the problem at hand. For this particular study, the adsorption model used (Equation 1) has been developed from experimental tests with field materials (soil and leachate) and calibrated – as reported previously by Yong and Samani (1987).

$$S_j^{ad} = E_j - B_j \quad exp(-A_j c_j) \tag{1}$$

where: E_j, B_j and A_j are soil parameters for component j to be determined from calibration experiments.

In a multi-component electrolyte solution soil system, mass conservation shows that the net desorption rate of a component species can be expressed as follows:

$$\frac{\partial S_i^{net}}{\partial t} = \frac{\partial S_i^{d}}{\partial t} - \frac{\partial S_j^{ad}}{\partial t} \tag{2}$$

where:

$\frac{\partial S_i^d}{\partial t}$ = rate of desorption of component i due to ion exchange, i.e., due to adsorption of other ions;
$\frac{\partial S_i^{ad}}{\partial t}$ = rate of adsorption of the component i which takes place simultaneously with desorption.

Desorption is a stoichiometric reaction (Helffrich, 1962). Hence, $\frac{\partial S_i^d}{\partial t}$ could be expressed as follows:

$$\frac{\partial S_i^d}{\partial t} = \sum_{j=1}^{m} \frac{\partial S_j^{ad}}{\partial t}; \quad j \neq 1 \tag{3}$$

where

S_j^{ad} = adsorbed amount of component j; and
m = number of adsorbed components

Substituting Eq. 3 in Eq. 2 gives:

$$\frac{\partial S_i^{net}}{\partial t} = \sum_{j=1}^{m} \frac{\partial S_j^{ad}}{\partial t} - \frac{\partial S_i^{ad}}{\partial t} \tag{4}$$

Substituting Eq. 1 into Eq. 4 yields:

$$\frac{\partial S_i^{net}}{\partial t} = \sum_{j=i}^{m} A_j B_j e^{A_j C_j} \frac{\partial C_j}{\partial t} - A_i B_i \quad e^{A_i C_i} \frac{\partial C_i}{\partial t} \tag{5}$$

Eq. 5 represents the general adsorption/desorption equation in a multicomponent solution system. Yong and Samani (1987) have shown that the one dimensional solute transport phenomenon can be expressed by the following equation:

$$\begin{aligned} &\frac{\partial C_i}{\partial t} + \left(\frac{K_{ch}}{K_h} + 1\right) V_z \frac{\partial C_i}{\partial z} + \frac{K_{ch} K_{hc}}{2K_h} \frac{\partial^2 C_i^2}{\partial z^2} \\ &= abe^{ac} \left(\frac{\partial C_i}{\partial z}\right)^2 + be^{ac} \left(\frac{\partial^2 C_i}{\partial z^2}\right) \pm \frac{\rho_s}{n} \frac{\partial S_i^{net}}{\partial t} \end{aligned} \tag{6}$$

Substituting Eq. 5 by the source term in Eq. 6 yields the general solute transport equation,

$$\begin{aligned} &\frac{\partial C_i}{\partial t} + \left(\frac{K_{ch}}{K_h} + 1\right) V_z \frac{\partial C_i}{\partial z} + \frac{K_{ch} K_{hc}}{2K_h} \frac{\partial^2 C_i^2}{\partial z^2} = abe^{ac} \left(\frac{\partial C_i}{\partial z}\right)^2 \\ &+be^{ac} \left(\frac{\partial^2 C_i}{\partial z^2}\right) \pm \frac{\rho_s}{n} \left[\sum_{j=i}^{m} A_j B_j e^{A_j C_j} \left(\frac{\partial C_j}{\partial t}\right) - A_i B_i e^{A_i C_i} \left(\frac{\partial C_i}{\partial t}\right)\right] \end{aligned} \tag{7}$$

APPLICATION

The results from the experimental study reported previously by Yong et al (1987) are used for application of the model. It is recalled that this study concerned contaminant migration through a sanitary landfill natural clay barrier (at Lachenaie, east of Montreal), and that the leaching column tests were performed using the leachate obtained from the collection wells – on the clay soils obtained in the region. The soil and leachate characteristics are summarized in Tables 2 and 3. The analyses concerning heavy metal adsorption have been reported by Yong et al (1987) and will not be dealt here. Foccusing on the cations Ca^{+2}, Mg^{+2}, and Na^{+} as the components involved in adsorption/desorption reactions, we observe that since, Ca^{+2} and Mg^{+2} are divalent cations, with a higher adsorption affinity than the monovalent cations Na^{+}, replacement of Na^{+} originally in the clay soil system should occur – i.e. desorption of Na^{+} occurs. This is confirmed by the breakthrough curve shown in Figure 1, where it is noted that at the 80-day period, the effluent concentration of Na^{+} is more than three times the influent concentration.

Using Eq. 5 to analyze Na^+ desorption, one obtains:

$$\frac{\partial S_1^{net}}{\partial t} = A_2 B_2 \quad e^{A_2 C_2} \frac{\partial C_2}{\partial t} + A_3 B_3 \quad e^{A_3 C_3} \frac{\partial C_3}{\partial t} A_1 B_1 e^{A_1 C_1} \frac{\partial C_1}{\partial t} \tag{8}$$

where the subscripts 1,2, and 3 refer to Na^+, Ca^{+2}, Mg^{+2} respectively. A_2, B_2, A_3, and B_3 coefficients must be determined from calibration of the experimental data for Ca^{+2} and Mg^{+2}. Also, $\frac{\partial C_2}{\partial t}$ and $\frac{\partial C_3}{\partial t}$ for all time steps can be calculated from the indicated calibration data using the finite difference technique as a method of solution.

Substituting Eq. 8 in the source term of the one dimensional solute transport equation (Eq. 6), the governing equation for Na^+ can be given as follows:

$$\left[1 - A_1 B_1 e^{A_1 C_1}\right] \frac{\partial C_1}{\partial t} + \left[\frac{K_{ch}}{K_h} + 1\right] V_z \frac{\partial C_1}{\partial z} + \frac{K_{ch} K_{hc}}{2K_h} \quad \frac{\partial^2 C_1^2}{\partial z^2}$$

$$= abe^{aC_1} \left[\frac{\partial C_1}{\partial z}\right]^2 + be^{aC_1} \frac{\partial^2 C_1}{\partial z^2} - \frac{\rho_s}{n} \left[A_2 B_2 \quad e^{A_2 C_2} \frac{\partial C_2}{\partial t} + A_3 B_3 \quad e^{A_3 C_3} \frac{\partial C_3}{\partial t}\right] \tag{9}$$

PARAMETER DETERMINATION

From leaching cell experiments (Yong et al. 1987), the concentration at different depths and times for the samples in the cells were measured. At the same time, concentrations at the same depth, and times are calculated for chosen parameters using the numerical method heretofore described. If the measured concentrations and calculated concentrations are designated as $C_{exp.}(z,t)$ and $C_{cal.}(z,t)$ respectively, then the best choice of parameters is that which minimizes the following functions:

$$\sigma = \sum_{i=1}^{M} ABS\left[C_{exp.}(z,t) - C_{cal}(z,t)\right] \tag{10}$$

where M is the number of measured concentrations in experiments. To minimize the above function, Powell's conjugate direction method in nonlinear optimization (Powell, 1964) is used.

The input data required in the computer program for parameter determination is the concentration profiles at all time steps. Thus for example, in the case of desorbed ion analysis, concentrations of the adsorbed ions involved in the problem at all time steps should first be obtained, to determine $\frac{\partial C_i}{\partial t}$ given in Eq. 5.

For the problem concerned with the Lachenaie landfill, concentrations of Ca^{+2} and Mg^{+2} were determined at all time steps, using the calibration computer program concerned with adsorption. Following this, their derivatives with respect to time $\frac{\partial C_2}{\partial t}$ and $\frac{\partial C_3}{\partial t}$ at all time steps were calculated, using the finite difference approximation method, and subsequently utilized in the calibration computer program concerned with sodium ion desorption.

The parameters obtained (Table 4, using the breakthrough curves shown in Figures 1 through 3) can be used in predictions of field performance – with the aid of the one-dimensional relationship given in Eq. 9. However, before sodium migration analysis can be performed, analyses for migration of calcium and magnesium must be obtained, as shown in Figures 4 and 5.

From the sodium concentration profiles after 200, 400 and 600 years shown in Figure 6, it is observed that the high concentration front travels propagates downward. This is consistent with expectations since sodium desorption in the initial layers of clay soil will continue to augment the sodium concentration in the lower layers – as migration of the contaminant front continues. The equal balance between effluent and influent concentrations occurs when mass exchange is satisfied – hence the tail end of bell-shaped curve, i.e. effluent sodium concentration equals influent concentration.

CONCLUDING REMARKS

The model developed in this study has been designed to address contaminant transport in saturated clays in a fashion which permits recognition of the physical fact that adsorption/desorption mechanisms exist in such systems. The transport coefficients are seen to be variables which depend on the initial system chemistry and the chemistry and concentration of the influent contaminant leachate solute.

The performance predicted using the developed model, for the tests conducted by Yong et al. (1987), shows that good accord is obtained between predicted and measured values – as shown in the laboratory situation reported by Yong and Samani (1987). Whilst it is not possible to validate the predictions for field performance for the 200 year plus period, it is expected that the "predicted" profiles will contribute a better appreciation to the evaluation of transport of the adsorbed/desorbed contaminant problem.

ACKNOWLEDGEMENTS

This study was conducted with support from the Natural Sciences and Engineering Research Council (NSERC Grant No. A-882) and the Quebec Ministry of Eductation (FCAR).

REFERENCES

Crooks, V.E., and Quigley, R.M. (1984) **"Saline Leachate Migration through Clay: A comparative Laboratory and Field Investigation"** Canadian Geotechnical Journal, vol. 21, pp. 349-362.

Grim, R.E. (1953) **"Clay Mineralogy"** McGraw-Hill, New York, 269 p.

Helfferich, F. (1962) **"Ion Exchange"** McGraw-Hill, New York,

Powell, M.J.D. (1964) **"An Efficient Method for Finding the Minimum of a Function of Several Variable without Calculating Derivatives"** Computer Journal, Vol. 7, pp. 1655-162.

Rowe, R.K., Caers, C.J., Booker, J.R., and Crooks, V.E. (1984) **" Pollutant Migration through Clay Soils: Observed and Predicted Behavior"** Geotechnical Research Report GEOT-6-84, Faculty of Engineering Science, the University of Western Ontario.

Stumm, W. and Morgan, J.J., (1970) **"Aquatic Chemistry: An Introduction Emphasizing Chemical Equilibria in Natural Waters"** Wiley Intersciences, John Wiley and Sons, New York, 583p.

Weber, W.J., (1975) **"Physicochemical Processes for Water Quality Control"**, Wiley Intersciences, John Wiley and Sons, New York, 640p.

Wiklander, L. (1964) **"Cation and Anion Exchange Phenomena"** Chemistry of Soil, 2nd , Ed., Ed. F.E. Bear, American Chemical Society, Reinhold, New York.'

Yong, R.N, and Samani, H.M.V. (1987) **"Modeling of Contaminant Transport in Clays Via Irreversible Thermodynamic "** Proceedings of Geotechnical Practice of Waste Disposal 87/GT Div. ASCE/Ann Arbour, MI, pp 846-860.

Yong, R.N., Warith, M.A., and Boonsinsuk, P. (1987) **"Migration of Leachate Solution through Clay Liner and Substrate"** ASTM, Special Technical Publication 933, pp 208-225.

Yong, R.N., and Warkentin, B.P. (1975) **"Soil Properties and Behaviour"**. Elsevier Scientific Publishing Co., Amsterdam, 449p.

Yong, R.N., Warkentin, B.P., and Mohamed, A.M.O.. (1990) **Principles of Contaminant Transport in Soils**, Elsevier Scientific Publishing Co., Amsterdam, *To appear.*

Table 1
Features of physical adsorption and chemisorption

Physical Adsorption	Chemisorption
Low heat of adsorption (<2 or 3 times latent heat of evaporation)	High heat of adsorption (>2 or 3 times laten heat of evaporation)
Non Specific	Highl specific
Monolayer or multilayer. No dissociation of adsorbed species. Only significant at relatively low temperatures	Monolayer only. May involve dissociaiton. Possible over a wide range of temnperature
Rapid, non-activated reversible. No electron transfer although polarization of sorbate may occur	Activated, may be slow and irreversible. Electron transfer leading to bond formation between sorbate and surface

Table 2
Soil characteristics/properties

Characteristics/properties	Values
Liquid limit	65%
Plastic limit	26%
Specific gravity	2.67
Void ratio	0.9
Dry Density	1390 Kg/cu. m.
CEC - cation ex. capacity	60 meq/100g
Permeability coeff. k	10*(-9) m/s
D50 (50% passing)	0.8 micro m.
D10 (10% passing)	0.1 micro m.

Table 3
Leachate characteristics

Parameter	Concentration (mg/l)
Calcium, Ca	180
Magnesium, Mg	35
Sodium, Na	140
Potassium, K	16
Zinc, Zn	2.5
Lead, Pb	1
Copper, Cu	1.7
Total iron	5
Chloride, Cl	190
HCO3	303
BOD	450
COD	860
TOC	190

Table 4

Parameters determined by calibration of experimental data

Solute component	a (mm^2/day)	b (g^{-1})	A (g^{-1})	B (g/g)	K ($mm^5/g/s$)
Ca^{+2}	23.65	-50,000	2588	0.001	-10,661
Mg^{+2}	236.0	-3000	1800	0.00071	-10,400
Na^{+}	84	-7,440	54	0.02928	-9,000

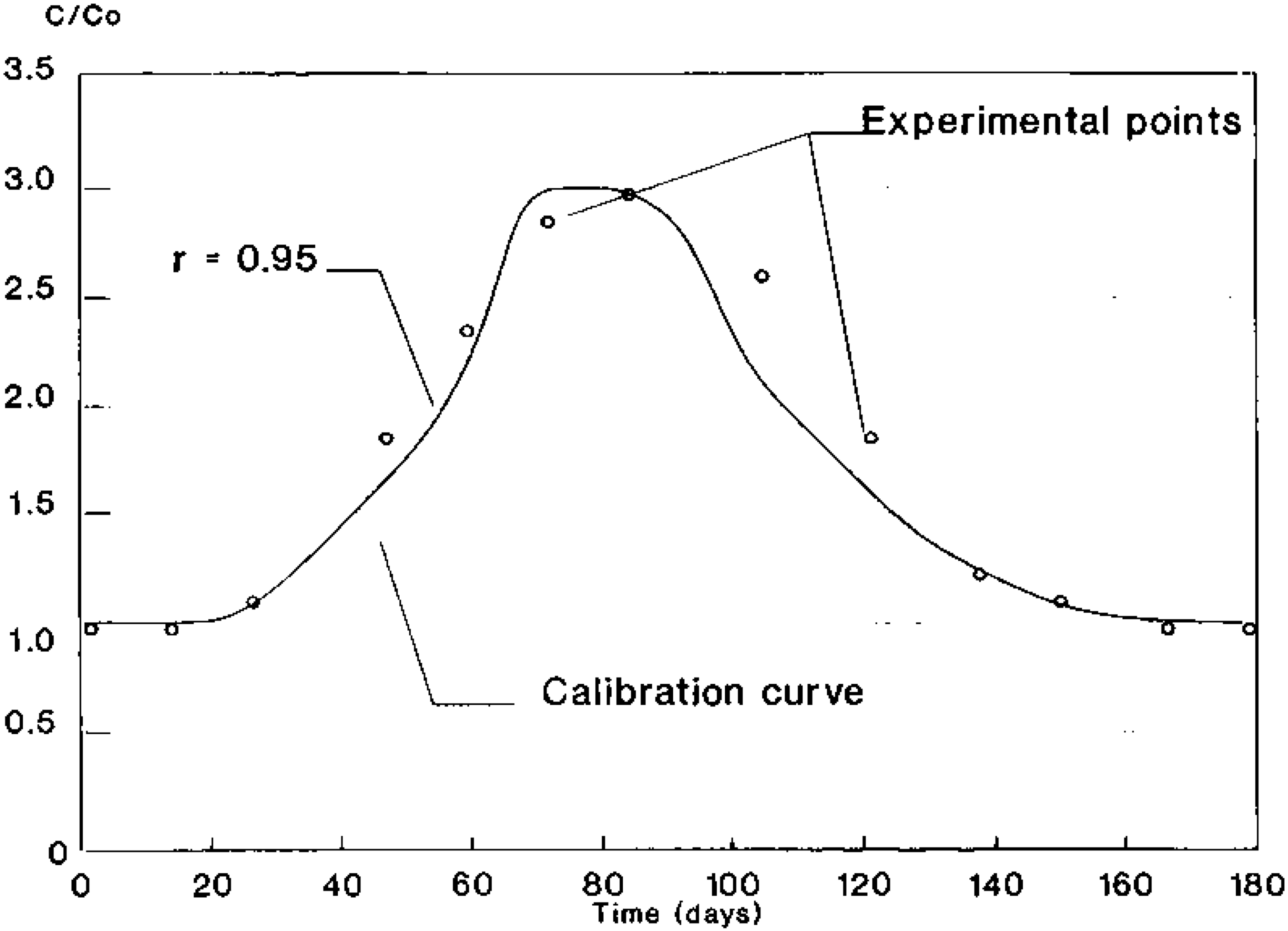

Fig. 1 - Sodium Calibration/Breakthrough Curve

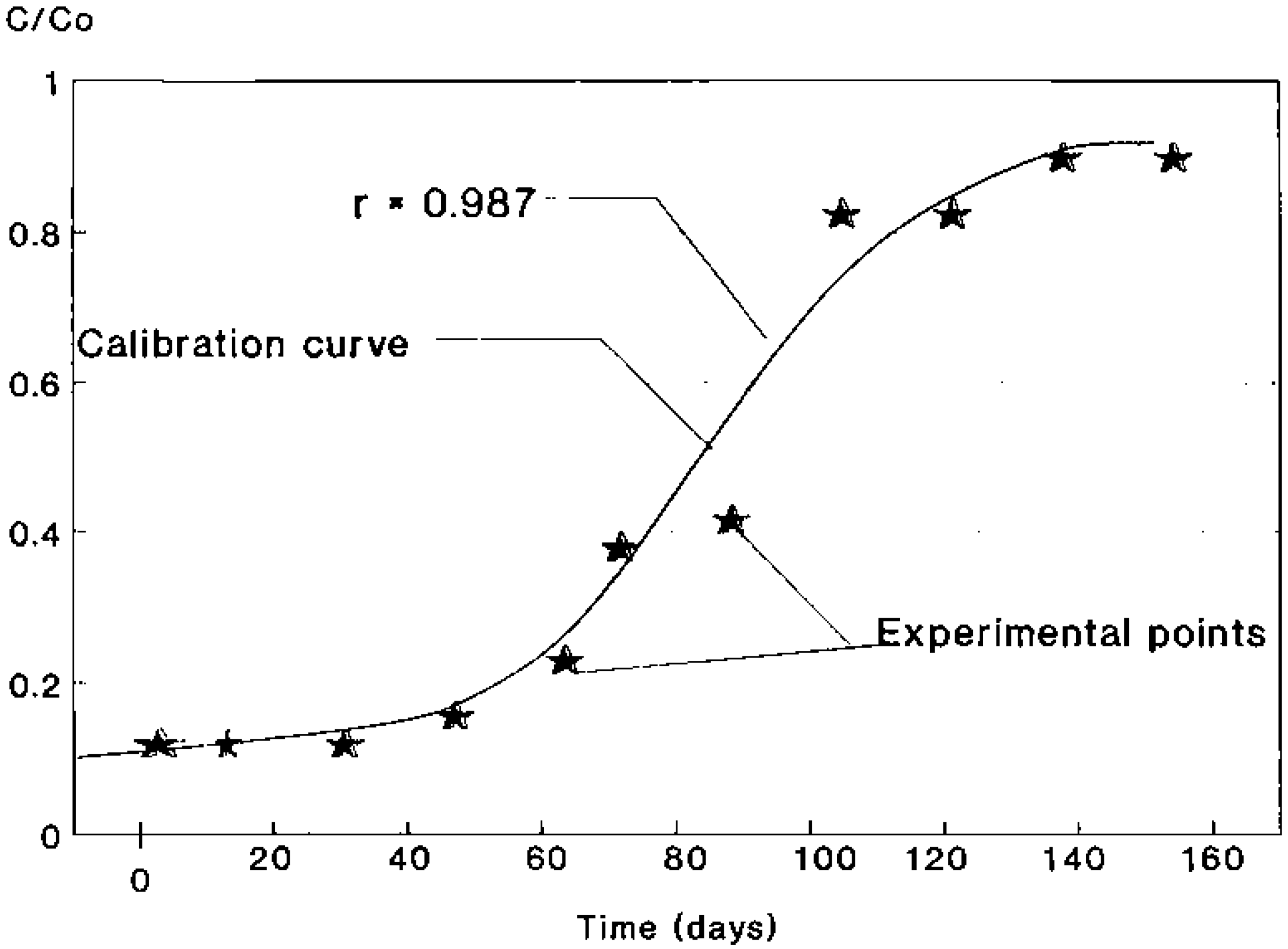

Fig. 2 - Calcium Calibration/Breakthrough Curve

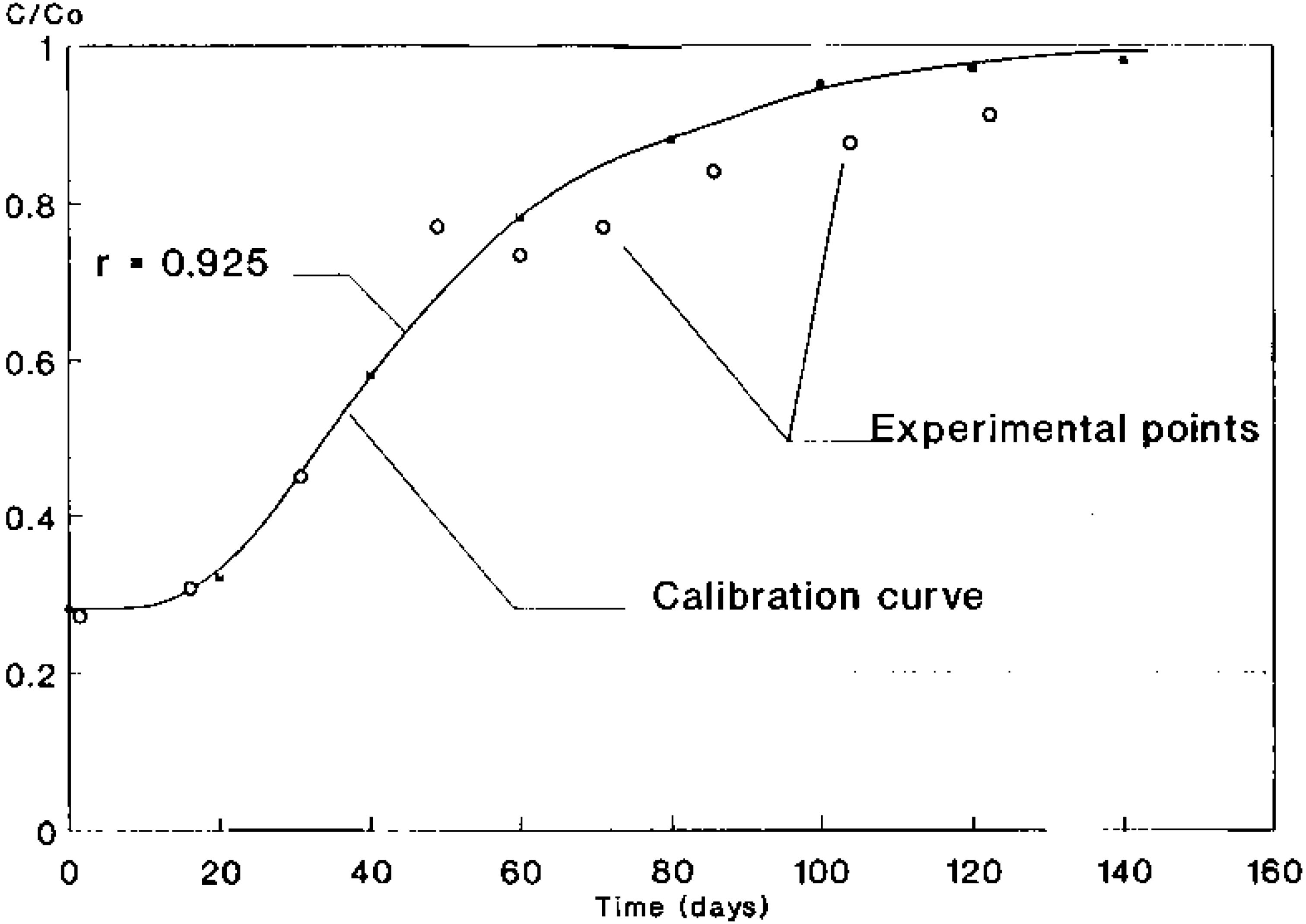

Fig. 3 - Magnesium Calibration/breakthrough Curve

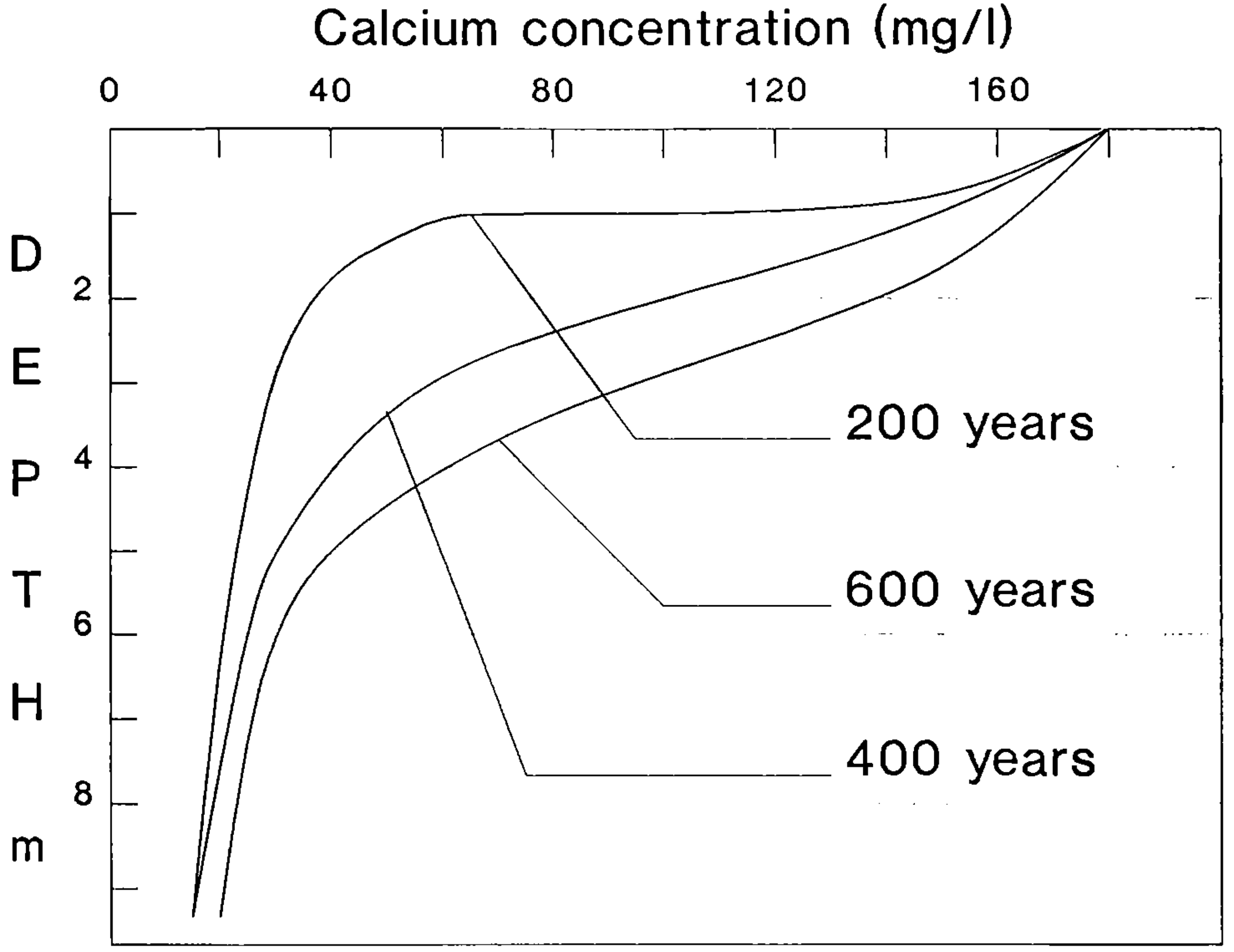

Fig. 4 - Calcium Concentration Variation with Time

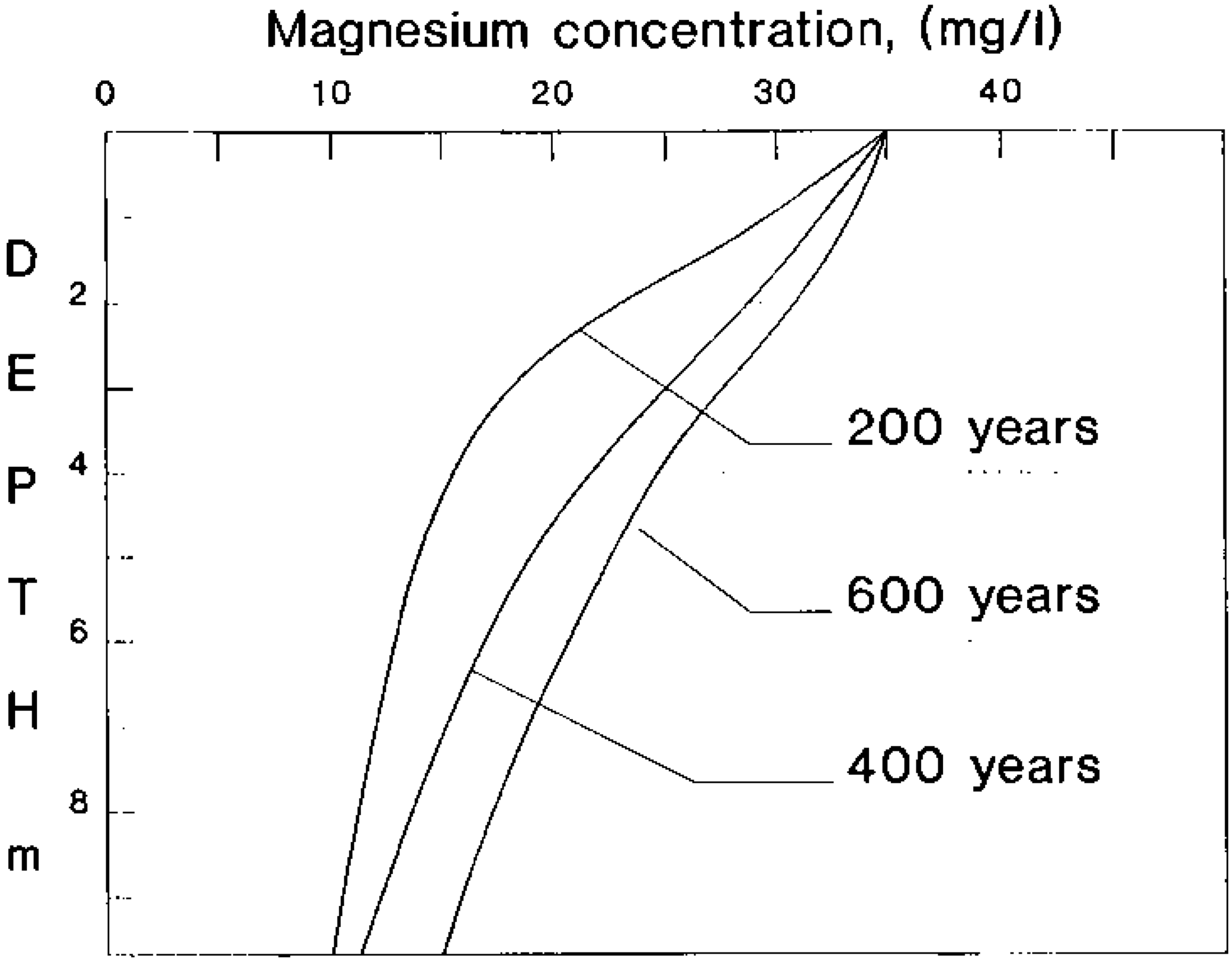

Fig. 5 - Magnesium Concentration Variation with Time

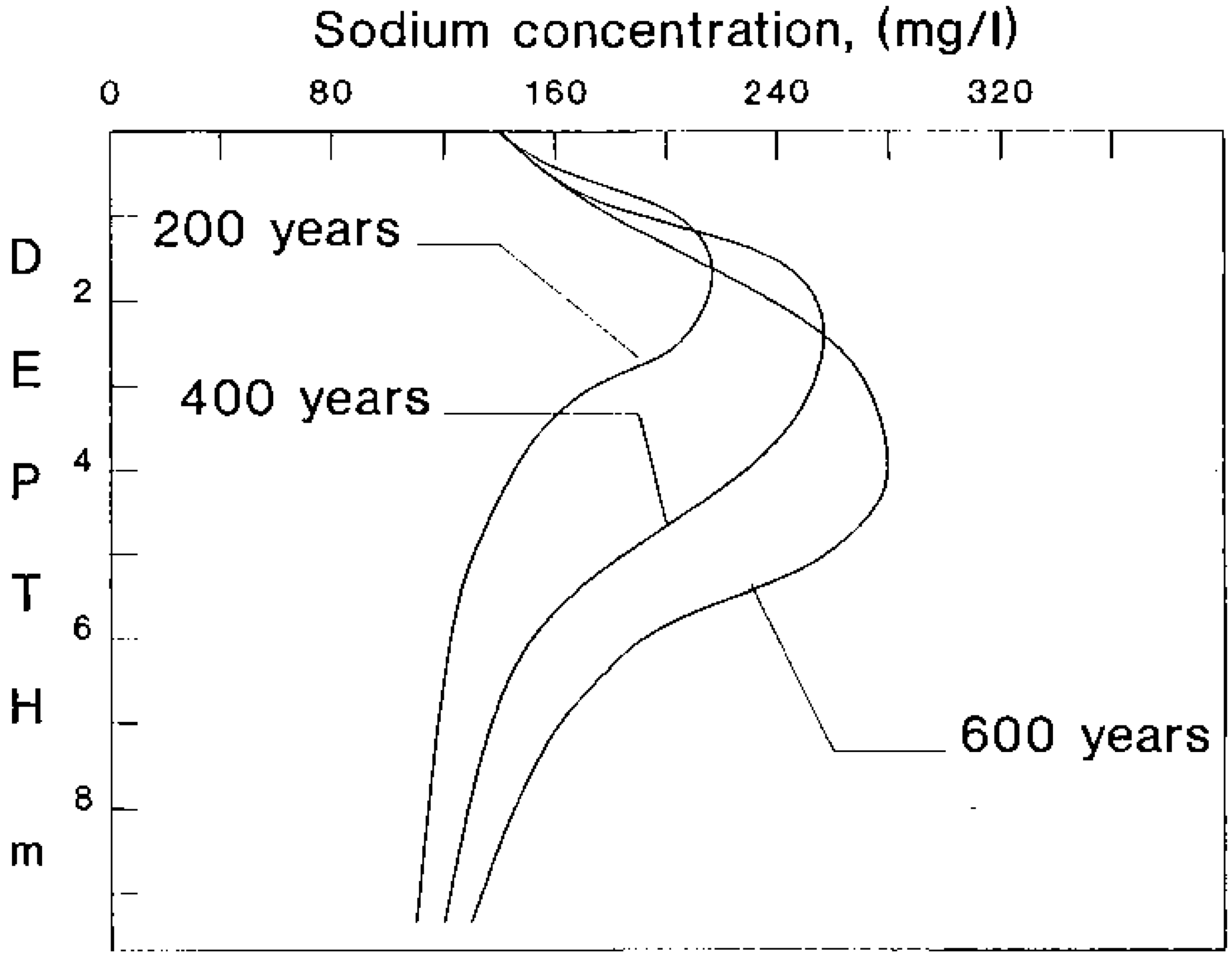

Fig. 6 - Sodium Concentration Variation with Time

SELF SEALING OF AERATED STABILIZATION BASIN FOR BLEACHED KRAFT WASTEWATER SLUDGES

RAYMOND N. YONG[1] AND MICHAEL C. CHEN[2]

Abstract

This study investigates the possibility of using the bleached kraft wastewater sludges as a sealant for basin containment of the sludges. Of the mechanisms of sludge self-sealing which include physical, physico-chemical, biophysical, and biophysico-chemical types (of seals). Particular attention was paid to the physico-chemical types. The set of criteria used to evaluate the capability of the liners developed include permeability, stability of the liner created, effect of changes in pH of the contained material, and hydrostatic pressure effects. The physico-chemical types of seals were found to be effective, and the coefficient of permeability was reduced by four orders of magnitude – between initial sludge formation and sludge cake development. Alum was chosen as a coagulant for forming the sludge layer for physico-chemical sealing. Stability analyses showed that under hydrostatic pressures and high pH ranges, the reduced permeability obtained in the sludge cake could be compromised if cracking occurs However, with the addition of sodium silicate and sodium aluminate, the alumino-silicate alum sludges appear to be more stable.

Key Words

Bleached Kraft Mill Effluent (BKME), self sealing, alum, coagulated BKME, physico-chemical sealing, Bingham yield stress, sodium silicate, sodium aluminate, permeability reduction, alumino-silicate.

---

[1] Geotechnical Research Centre, McGill University

[2] Formerly Geotechnical Research Centre, *deceased*

Introduction

In the pulp and paper industry, the treatment of effluents to reduce BOD to acceptable levels prior to discharge to receiving waters is generally accomplished with the aid of holding ponds where these effluents can be treated for removal of the dissolved organics by aeration. The choice of a proper "impermeable" basin (pond) liner system to prevent leakage of the contained effluents and to protect the substrate groundwater environment from contamination from the contents of the aerated stabilization basin (ASB) is critical. Given the choices between synthetic (plastic) liners, cement and asphalt grouting systems, clay engineered barriers, and liners developed through self-sealing mechanisms, it is clear that if self-sealing mechanisms can be made to work, these would result in considerable economic benefit to the Industry.

To develop a self sealing membrane from the sediment formed from the settling solids in the contained effluent, several opportune events have to occur to permit the sediment to act as an impermeable membrane. These relate to (a) the composition and properties of the suspended solids, (b) the nature of the interactions between the solids, (c) the need for treatment of the suspended solids (or suspension) to promote beneficial interaction, (d) the developed rate of sedimentation of the suspended solids, (e) the developed properties of the initial sediment, (e) the consolidation rate of the sediment, and (f) the stability of the final sediment membrane or sludge cake.

To determine the possibility of developing a self-sealing membrane from bleach kraft mill effluents (BKME), the laboratory study reported herein considered the following:

1. Compositional characterization of BKME solution and the initial substrate material,
2. Capability of the untreated BKME to develop self sealing properties,
3. Determination of the optimumn coagulant dosage to induce beneficial precipitation of the BKME, and
4. Filtration-permeability tests for evaluation of the permeability reduction of the sludge sealing system.
5. Long term stability of the sludge blanket/cake.

Induced Sludge-Sealing Process

The different possible processes involved in the development of membrane seals from tailings waste disposal are shown in Figure 1 – for the types of waste discharge with characteristics and properties amenable to membrane sealing formation. The three basic categories are identified via source material, e.g. non-coagulated BKME, coagulated BKME, and fluid phase of BKME as initiator of swelling in the soil basin lining. In the last category, one relies on the interaction of the fluid phase (chemistry) with the soil constituents to produce swelling in the soil constituents such that void plugging occurs – hence permeability reduction is achieved, and a proper impermeable clay lining is obtained.

In regard to the other two categories, coagulated and non-coagulated BKME, on relies on the interaction and settlement of the suspended solids of the BKME (sludge or sludge cake) to form a "coating" (layer) that would be impermeable. The key elements in the system relate to the capability of the settled untreated or treated sediment to form an impermeable membrane in the time-frame consistent with economic waste treatment and disposal requirements. In this study, the physico-chemical approach using the coagulated BKME (3rd. column in Figure 1) was chosen. Accordingly, the procedures for investigation included the following considerations:

Steps leading to physico-chemical type of sealing

STEP 1 – untreated coagulation/flocculation of suspended solids from wastewater.
STEP 2 – settling-filtration of the suspended solids on the pervious soil base.
STEP 3 – filter caking and consolidation of an impermeable layer of sludge.
STEP 4 – final physico-chemical type of sealing of the pervious soil base.

Process for alum coagulated solid system induced sealing

STEP 1 – alum treatment for coagulation of BKME suspended solids.
STEP 2 – settling-filtration of coagulated solids on the pervious soil base.
STEP 3 – addition of other chemicals to improve sealing efficiency and stability.
STEP 4 – void plugging and sludge caking on soil filter medium.
STEP 5 – consolidation of sludge filter cake.

STEP 6 - final physico-chemical type of sludge sealing.

In the general design/construction requirements for an impermeable basin liner system, one tries to use a material which would not permit passage of the fluid contained in the basin. If a clay barrier is used, the normal procedure would be to use a compacted clay with minimum permeability coefficient k of 10^{-7} cms/sec. However, if a seal could be formed from the wastewater (effluent) being contained in the pond - using the properties of settled solids (perhaps enhanced by some process introduced into the system) - the costly preparation required to provide an impermeable base might be avoided. If self sealing could work, one would be able to utilize the natural sub-base which might indeed have k values considerably higher than the 10^{-7} values.

The procedure used in this study to evaluate the capability of self sealing to produce the resultant liner requirements, involved the use of a pervious sand blanket overlying a more impervious base. This situation permits gradual filling and "blocking" of the pore spaces (sludge penetration) in the sand blanket during settling of the sludge solids, followed by a build-up of a sludge layer atop the in-filled sand blanket. The resultant in-filled sludge formation is considered an "in-depth cake". If a further sludge layer forms on top of the in-filled sand blanket, the process leading to the development of the combined sludge layer can be identified as an in-depth and cake filtration process. Whilst the mechanisms leading to enhancement of cake formation are not well known or understood, it is considered likely that if stabilization procedures can be developed, the permeability of the resultant cake could meet the requirements for liner barriers.

Experimentation

To permit efficient evaluation of the capability of the treated BKME system to produce self sealing properties, the sand blanket was used by itself - without benefit of the underlying clay subbase. The basic test for evaluation consisted of the *permeability reduction* test, using the settling column system shown in Figure 2, in conjunction with a variable speed drive system to provide the BKME input to the column, and a two-way valve attachment at the bottom of the column to permit atmospheric venting or vacuum extraction. The testing procedures permitted with the system combines a soil-column settling test with a subsequent permeability test when atmospheric venting if permitted at the bottom of the sludge cake. Whilst this does not necessarily mirror the field situation of sedimentation, it permits a quick study of the capability of the treated BKME to develop sealing of the sand, under conditions which are considerably more adverse that in the field. In using the set-up shown in Figure 2 for permeability testing, the Masterflex variable speed drive, model 7545-00, series 70/3 recirculation pump is used to provide a constant head. The basic steps of the experimental study consisted of:

- Charaterization of the soil (sand) and the BKME (permeant).
- Tests of the BKME for determination of optimum alum dosage.
- Permeability reduction tests for the various treated BKME.
- Stability tests of the sludge cakes.

Sand (cover material) and BKME

Preliminary tests for evaluation of the types of sand to be used involved assesment of the permeability of the sands tested. The sands examined were silicate sand with different gradations and maximum size: #70, #24 and #16. The D_{50} grain size k values obtained from falling head permeability tests are given in Table 1, together with the characteristics of the BKME used for the experiments[3]. Inasmuch as the #24 sand represented the "mid-range", it was decided to use this as the sand blanket material for the settling column tests - and also for evaluation of capability of the sludge to penetrate into the sand and to develop an effective "cake".

Four different batches of BKME (15 gallons per batch) were received at various times - during the course of the study. Because of various circumstances, the pH variation between the batches was much higher than the compositional variations observed between the batches. Values of from 7.2 to 11.5 in pH were obtained between the different batches. Thus, for the tests conducted, most of the detailed tests were conducted on the batch containing the higher pH value - principally because this batch was received during the "critical" period of detail testing. The other batches, received at various times, were

---

[3] The BKME used was obtained from Consolidated Bathurst Inc. Portage du Fort, Quebec, courtesy of Mr. A. Lafleur.

evaluated for composition, and other "spot" tests – e.g. settling tests, permeability, alum dosage requirements. Hence, in the reporting of test results, the values shown are specific to the BKME with an initial pH value of about 11.5. Reference to the other batches of BKME, with different initial pH values will be made at various times – with specific identification to the initial pH condition.

Coagulant – Alum

Since previous experience with the use of alum in the primary treatment (reaction clarifier) of effluents in the pulp and paper industry (Chen, 1974) have shown considerable success, it was decided to use alum as the coagulant for this study. In the presence of the kind of alkalinity shown in Table 1, (290 mg/l), the chemical reactions that would occur when alum is added to the BKME could include:

$$Al_2(SO_4)_3 + 3Ca(HCO_3)_2 \longrightarrow 3CaSO_4 + 2Al(OH)_3 \downarrow + 6CO_2 \uparrow \tag{1}$$

$$Al_2(SO_4)_3 + 6NaOH \longrightarrow 3Na_2SO_4 + 2Al(OH)_3 \downarrow \tag{2}$$

Soil column and permeability tests

The dosages of alum added to the BKME ranged from 400 mg/l to 1,400 mg/l – applied in increments of 200 mg/l.

In using the test system shown in Figure 2, it was important to ensure that in filling the the soil column such that the bottom sand blanket was not disturbed. This was accomplished by first saturating the soil column with distilled water, and filling the column with distilled water to a height of about 5 to 7 cms above the surface of the sand blanket. When the BKME was introduced into the soil column, the feed nozzle was arranged such that it fed the material to the wall of the column, thus minimizing the disturbance effect. In addition, the rate of feed of the BKME was continually adjusted such that the efflux time of the initial liquid (from the column) was approximately the same as the feeding time. When the initial liquid (water) was total replaced by the BKME, the settling column was filled up to a height of about 25 cm above the sand filter surface – to commence the settling experiment.

For determination of the permeability of the sludge cake, five piezometers were installed along the wall of the soil column - in a vertical line, at heights of 0.95cm, 0.16 cm, above the sand filter, 0 cm (on the surface), and 0.64 cm and 8.6 cm below the surface of the sand filter surface, - as shown in Figure 2. The coefficient of permeability of the sludge cakes were calculated on the basis of measurements of pressure drops across the different layers, the filtration rate, the assumed concentration profile within the cake, and the amount of penetration of the sludge into the sand filter.

Results and Discussion

The settling column tests showed the characteristic maximum settling rates at the initial stages of sedimentation of the solids - decreasing rapidly after the second hour of sedimentation. Using light transmission through the midpoint of the supernatant (at a $450\mu m$ wavelength) for comparison, one can compare the efficiencies of the various dosages of alum in regard to settling rate and characteristics. Figure 3 shows the results of transmission tests, conducted after a 10-minute elapsed time, (i.e. 10 minutes after start of settling test). The pH value of the alum BKME mixture is also given, together with the tests on a corresponding "blank" (i.e. at 0 alum dosage). Note that the light transmission values are given in terms of the logarithmic value of the percent light transmission through the supernatant. Thus, at 100% light transmission, the log. value should be 2. Similar types of "curves" can be obtained with the other batches of BKME received - where initial pH values are different.

As expected, increasing dosages of alum resulted in greater efficiency in settling of the suspended solids. Whilst one would be tempted to increase the dosage of alum to continue increasing the efficiency of settling, it should be noted that at an alum dosage of 1,600 mg/l (not reported in this paper), the alum-BKME coagulated mixture produced a sludge that was so massive that zone settling was virtually denied. It should be mentioned that the initially high pH value of the "blank" was due to the fact that the samples received for study did not undergo neutralization after biological treatment (refer to 3rd column in Figure 1). The influence of different values of initial BKME pH on alum dosage requirements must be stressed as one of the factors that needs to be studied if one wants to apply alum treatment to the field situation. Since the effluents will always be variable in nature, it is expected that the pH will vary correspondingly. Since alum reacts with the alkalinity of the BKME to produce aluminium hydroxide complexes which are adsorbed by the colloids as part of the agglomeration process, it would be most advantageous (in practice) to obtain the BKME at a pH value close to 7 if one wishes to decrease the alum dosage.

A comparison of the equilibrium sludge heights as a function of alum dosage for the period of 2 days and 25 days of sedimentation is given in Figure 4. Maximum sludge height is apparently obtained with the 1000 mg/l alum dosage. The "consolidation" of the sludge over the 2 to 25 day period is evident from the decrease in sludge height between the 2 to 25 day period. In other tests conducted to determine the relationship between maximum sludge height and initial pH of the BKME, it was shown that for the BKME's with initial pH values of 7.0, 9.5, 10.5, and 11.5, the maximum sludge heights obtained were: 250 mg/l, 700 mg/l, 1000 mg/l, and 1,600 mg/l, respectively.

The rheogram analyses, performed with a rotating cylindrical viscometer, Contraves Rheometer 5, confirmed that the sludges (treated and untreated) could be classified as non-Newtonian. By projecting the linear portion of the rheogram onto the shear stress axis, the Bingham yield stress τ_B for each sample tested was obtained. The results of the analyses are also shown in Figure 4 - indicating that the 1000 mg/l alum dosage produced the highest Bingham yield stress.

The material balance for the alum coagulated BKME system shown in Figure 5 indicates the amount of solids in the sludge and supernatant. The values shown are cumulative, e.g. the total solids content of the actual alum-BKME mixture at 400 mg/l is 1160 mg/l. This includes the solids concentration in the supernatant and in the sludge. Note that the solids concentration in the supernatant (870 mg/l) includes 350 mg/l organics. The total solids content was obtained from oven-dried samples of both the supernatant and the settled sludges at 110^{0}C over a 12 hour period. The solids concentrations are expressed as the weight of solids per total volume (mg/l) of solution. This is obtained by multiplying the solids concentration of either the supernatant, or the sludge, by its individual volume, and dividing by the total volume. The solids in the supernatant are also considered in terms of the organic solids contribution to the total. In this case, determination of the organic solids content was obtained by drying to 650°C. It is interesting to observe that the organics solids concentration decrease with initial addition of alum, but increases after the concentration of alum begins to exceed about 800 mg/l.

Evolution of Sludge Sealing Process

To obtain an appreciation of the sludge sealing process, it is useful to recount a typical settling column experience. One begins by recalling that the settling column has been previously filled with distilled up to a height of about 7 cms. above the surface of the sand blanket. The sand blanket is 10 cms. thick and is allowed to drain at the bottom - if the "vent" valve is opened. The alum coagulated sludge prepared in a 250 ml beaker is stirred before pouring into the settling column - following the procedure described previously. Referring to Figure 2 for the test set-up and corresponding piezometric pressure development, the results shown in Figure 6 correspond to the time steps described as follows:

* At time t_o = 0 secs., 250 ml of 630 mg/l of solids is poured into the settling column.
* At time t_1 = 20 secs., penetration of about 0.3 cms into the sand blanket (at the bottom of the settling column) is observed. Sludge thickness above the sand blanket surface is estimated to be about 0.2 cms. Above this, one observes a "thick" solids suspension. Because the bottom of the sand blanket is open to atmosphere, the initially saturated sand blanket drains and becomes unsaturated.
* At time t_2 = 250 secs., the piezometer beneath the sand (blanket) surface reads zero, and if one visualizes the pierometric pressure "curve" in terms of three "linear" segments - as shown in Figure 6 - it is possible to assume that the cake will show at least 3 different permeabilities (k_1, k_2, and k_3). The sludge penetrated layer in the sand blanket (lowest layer) is identified as the one providing the value of k_1. This is the lowest value, with k_2 and k_3 increasing in an almost linear fashion.
* At time t_3 = 350 secs., the build-up of the cake above the surface of the sand blanket has not really begun. Penetration of the settling solids into the sand voids is still active.

- At time t_4 = 970 secs., the piezometric pressure readings suggest that the penetration of the settling solids into the sand voids is almost complete, and that the relative dispersed nature of the solids above the sand surface is becoming more "compact".
- At time t_5 = 3150 secs., the developed sludge cake above the sand surface is about 0.7 cms. The 3 layers can now be considered as being reduced to 2 layers, – or even 1 layer.

Further observations will show that some consolidation of the sludge cake occurs, and that some deposition of aluminum hydroxide of the surface of the cake also occurs. The calculation of "permeabilities" from the piezometric heads and the outflow requires the determination of the velocities in the 3 "layers" (or two layers). One should note that the measurement of the "layer" thicknesses during the settlng process is never simple nor precise. Very often, no clear separation between layers can bd readily distinguished. Nevertheless, it is assumed that the information from the piezometric pressure profile can be used to assist the visual measurement technique for determination of thickness of the layer thicknesses.

Determination of the effective velocity v in each layer requires the application of the simple continuity condition:

$$v(cake) = \frac{v(sand) \cdot \epsilon(sand)}{\epsilon(cake)} \tag{3}$$

where ϵ represents the porosity of the sand or cake – as the case may be. Determination of ϵ(sand) is easily done with a knowledge of the amount of sand used to fill the 10 cm height of the settling column. However determination of the ϵ(cake) requires knowledge of the solids content in the layer in question. This is obtained by using the information obtained from the piezometric profile, and constructing a solids concentration profile as shown in Figure 7. The values of T-1 through T-5 shown in the Figure correspond to the t_1 through t_5 values discussed previously. The information obtained from calibration tests with light transmission values (such as those shown in Figure 3), and determination of solids concentration in the supernatant for correlation with light transmission values, are needed to ensure that the mass balance calculations used for Figure 7 are met.

With the values of v for the different layers, simple application of the Darcy model will provide the appropriate calculated permeability value k_n, where $n = 1, 2$, or 3. This form of analysis for permeability can be made throughout the settling process, at various t_n times. In this manner, the permeability reduction with time will be obtained. Figure 8 shows the results of the calculations for the various k values for the 1,400 mg/l alum addition to the BKME with the high initial pH – i.e. the test material reported in detail herein (Table 1). Because of the considerable difficulty in calculating the effective thickness of the second layer above the sand blanket (3rd. layer responsible for k_3), only two points are shown for the k_3 values. As time progresses, as shown in Figure 6, the layers become more compact and begin to be indistinguishable as distinct layers. Thus we note that at $t = 3150$ seconds and beyond, we can consider the cake to be one layer. Using the "total" cake system, we observe that the permeability reduction is four orders of magnitude – beginning from the 20 second sludge deposition.

Sludge Cake Stability

Assesment of the capability of the developed sludge cake to withstand hydrostatic pressure over a period of time required application of pressure tests to the sludge cakes developed in and above the sand blanket. It was observed that with a hydrostatic pressure of 45 kPa, some increase in the final sludge cake permeablity of the sludge cake was observed – even though visual observations did not show any further penetration of the sludge into the sand voids. Since this pressure is typical of the pressures in aeration ponds, it was decided to seek improvement in the "stability" of the sludge cake. This was achieved by performing a series of screening tests with additives used in conjunction with the alum. The primary sets of controls were related to permeability reduction and capability to withstand hydrostatic pressure without further penetration into the sand blanket and without any increase in permeability. The screening tests showed that a combination of sodium silicate and sodium aluminate could produce a beneficial effect when added to the alum.

Longterm solubility assesment required subjecting the sludge cakes to leaching assault with varying pH solutions of BKME. The combination of mechanical stability and solubility tests recognizes the situation that the alum-coagulated sludge cake which rests at the bottom (and sides) of the aeration lagoon is subject to attack from various chemical forces

– under a hydrostatic head. One needs to be concerned with the solubility of the aluminum hydroxide in the cake. Tests conducted to determine the distribution of solids in the typical cake show that about 25% of the cake material consists of porous fibres, and that the aluminum hydroxide content expressed as $Al(OH)_3$ varies between 7 to 50% depending on the initial pH of the BKME and the amount of alum added. Between 25% and 65% of the cake (depending on the fibres and $Al(OH)_3$ content) consists of other kinds of suspended matter, e.g. lignin complex and colloids. Determination of the solubility of the aluminum ion in the BKME solution is possible with the aid of the mass balance information – such as the one shown in Figure 5. By analyzing the contents of the supernatant (aluminum concentration), at various times and dosages of alum, one can produce a solubility diagram – thus permitting one to calculate the amount of time taken to dissolve the aluminum hydroxide in the alum-BKME sludge cake.

The solubility results obtained in relation to aluminum ion in the BKME solution showed that equilibrium solubility was obtained between $\mathrm{p}Al = 4.75$ and $\mathrm{p}Al = 4.0$ – (where $\mathrm{p}Al$ is -log Al^{+3} ions). Using a $\mathrm{p}Al$ of 4.75 and an average permeability of 2×10^{-8} cms/sec and a 7% $Al(OH)_3$ content in the cake, the time estimated to dissolve the cake was 60 years. However, should one assume the $\mathrm{p}Al$ to be 4.0, this time is reduced to 11 years. Since the calculations have to rely on several assumptions, further insight into the stability of the sludge cakes was sought from leaching tests which were conducted with both alum-BKME sludge cakes and the additive treated alum-BKME – i.e. addition of alumino-silicate to the alum-BKME. The leaching tests on the alum-BKME sludge cake samples were conducted with BKME at pH values ranging from 10 to 5.2, with the greater attention given to the ones with pH values around 7 – as representative of the field condition. Aluminum concentration was measured in both the influent and effluent during the leaching tests, and since the variables were initial pH of the BKME leachate solution, time and number of leaching pore volumes, it was possible to extrapolate the data to determine the time required for complete dissolution of the aluminum hydroxide in the sludge cake. One should be cautioned to recollect that in experimental determinations, the sources of Al are never fully identified, and thus extrapolation of such values for determination of dissolution efficiencies cannot be accepted will full confidence. Nevertheless, with recourse to the solubility results, the experimental results showed that for initial BKME leachate pH of about 6.5, the extrapolated time for dissolution of the cake ranged from 3 to 6 years. However, with an initial BKME leachate pH of from 7.3 to 7.7, the extrapolated time was shown to be between 5.5 to 20 years.

In the case of the sodium alumninate and sodium silicate addition to the alum-BKME, it is reasoned that the reaction between the sodium aluminate and sodium silicate would be advantageous, since both materials are highly alkaline in solution, and both remain individually depolymerized until the formation of alumino-silicate. The tests conducted in this study, with the alumino-silicate addition to the alum coagulated BKME can only be considered as preliminary. The reasons are manifold – mainly tied into the fact that proper detailing of the various reactions and result cannot be obtained. Experience shows that when a solution of polyvalent metal salt is mixed with a solution of a soluble alkali metal silicate, such as sodium silicate, an insoluble metal silicate is usually precipitated a gelatinous amorphous mass (Iler, 1955, Lang and Spencer, 1968). Most solutions of soluble silicates do not contain silicate ions of uniform size, but instead, a mixture of polysilicate ions. Since the polysilicate ions are not uniform in size, they cannot arrange themselves along with the metal ions into a regular crystal lattice. The result obtained is generally identified as an insoluble precipitate which is somewhat amorphous.[4] Iler (1955) states that the precipitation of a metal silicate from an aqueous solution at ordinary temperature does not yield crystalline silicates, but rather, results in a colloidal mixture which may be visualized as an adsorption of metal ions on the gelatinous silica or as a mutual coagulation of the positively charged colloidal metal hydroxide and negatively charged colloidal silica. In dilute solutions, since colloiodal metal silicates are precipitated at pH values slightly below that at which the metal hydroxide would be precipitated, no definite compounds are formed, and the hydroxides precipitated along with the silica are by mutual coagulation.

It is evident that the manner of mixing, the proportions used, and the other yet to be detailed factors control the kinds of amorphous inhomogeneous precipitate obtained. Focussing for the time being on the ratio of the sodium aluminate to the sodium silicate, – with everything else being held constant – eight samples were tested. The molar ratios

---

[4] If one wishes to obtain a crystalline silicate for better quality and stability, the polysilicate ions need to be depolymerized into small silicate ions of uniform size – to obtain a regular lattice.

varied from 0.12 to 0.84 – where the molar ratio is defined as $\frac{Al_2O_3}{(Al_2O_3+SiO_2)}$. The test results obtained by subjecting the alumino-silicate added alum-BKME sludge cakes to hydrostatic pressures of 56 kPa showed no deterioration in the value of permeabilities obtained. Further beneficial gain in the k values were obtained for the sample with the molar ratio of 0.12 – where increased penetration of the cake into the sand blanket was obtained under the hydrostatic pressure.

In the case of the leaching tests under a hydrostatic pressure of 56 kPa, the pH values of the leachate ranged from 10.7 to 5.7. Analysis of the effluent showed that the lowest Al^{+3} concentration was obtained with the sample with a molar ratio of 0.24 – even though the pH of the leachate was 9.9. Extrapolation for estimation of total time taken to dissolve the cake was not possible since the solubility relationships for the alumino-silicate alum-BKME mixtures were not available. These have yet to be performed. However, in view of the very low registration of Al^{+3} in the effluent at the high 56 kPa pressure leachate tests, it is expected that the total dissolution time would exceed that obtained for the alum-BKME sludge cakes.

Concluding Remarks

Whereas the alum-coagulated BKME test results have been reported herein to demonstrate that physico-chemical sealing (3rd. column in Figure 1) can be developed for BKME used, other types of sealing experiments were also conducted. For example, in the experiments conducted to examine feasibility of physical sealing (1st. column in Figure 1), it was shown that for the same BKME used, the coefficient of permeability was reduced from and average of 6.5×10^{-2} cm/sec to an average of 2.0×10^{-3} cm/sec in ten hours. After this time period, the reduction in k value was minimal. For that reason, there was no reason to continue evaluation of the feasibility of physical sealing.

Experiments conducted to study the other types of sealing identified as the second and fourth columns in Figure 1 showed good potential for sealing – within the same range of effectiveness as the physico-chemical type of sealing. However, because of the various difficulties in obtaining proper identification of the biological solids and their characteristics, the results will need to be reported at a later time.

The results from this particular study show promise in that self-sealing from the BKME can be obtained via physico-chemical processes without considerable cost and time. The permeability reduction obtained after 8 hours is encouraging, and needs to be tested in pilot field experiments where mass and local conditions are to be exploited. The choice of the particular concentration of alum to be used must be conditioned by the initial properties of the BKME – particularly pH. In the tests reported herein, the choice of the 1,400 mg/l concentration for alum addition was confirmed not only by the equilibrium sludge height development, but also by the peak Bingham yield stress point, and the clarification of the supernatant. A certain degree of "mechanical" stability of sludge cake is important.

Even though the tests indicate that the "life-span" for the sludge cake could be between 3 to 20 years (depending on the pH of the leachate), it should be noted that in the field condition, experience shows that biological activity within the system will promote increased stability of the sealing phenomenon. Experience shows that about 0.2 kg of biological solids are produced per kg of BOD reduction in these kinds of lagoons (Eckenfelder, 1967). However, if increased stability is sought, it is suggested that the addition of alumino-silicates to the system would contribute to the chemical stability of the coagulated mass.

Acknowledgement

Acknowledgement is made to the Natural Sciences and Engineering Research Council (NSERC – Grant No. A-882) and to the Quebec Department of Education (FCAR Grant) for support for this study. It is with considerable regret that the very untimely death of co-author Dr. Chen shortly after completion of the study did not permit him to pursue the considerable promise that lay ahead of him.

Bibliography

Chen, C. L., (1974), "Project Report on the Performance of Reaction Clarifier for Scott Paper Mill Ltd.", T. W. Beak Consultants Ltd.

Eckenfelder, W. W., (1967), "Comparative Biological Waste Treatment Design", Journal of the Sanitary Engineering Division, ASCE, Vol. 93, No. SA6, pp 157

Iller, R. K., (1955), "The Colloid Chemistry of Silica and Silicates", Cornell University Press, Ithaca, New York.

Lang, K. R., and Spencer, R. W., (1968), "On the Mechanism of Activated Silica Gel Formation", Environmental Science and Technology. Vol. 2, No. 3.

Table 1
Properties of BKME and Sand

Sand	Sand
#16 sand; D50 = 1.00 mm	k20 = 0.02 cm/sec
#24 sand; D50 = 0.42 mm	k20 = 0.08 cm/sec
#70 sand; D50 = 0.20 mm	k20 = 0.03 cm/sec
BKME	BKME
BOD	192 mg/l
COD	823 mg/l
Suspended solids	138 mg/l
Ca	14.9 mg/l
Na	123.8 mg/l
Mg	3.8 mg/l
Total alkalinity	290.0 mg/l

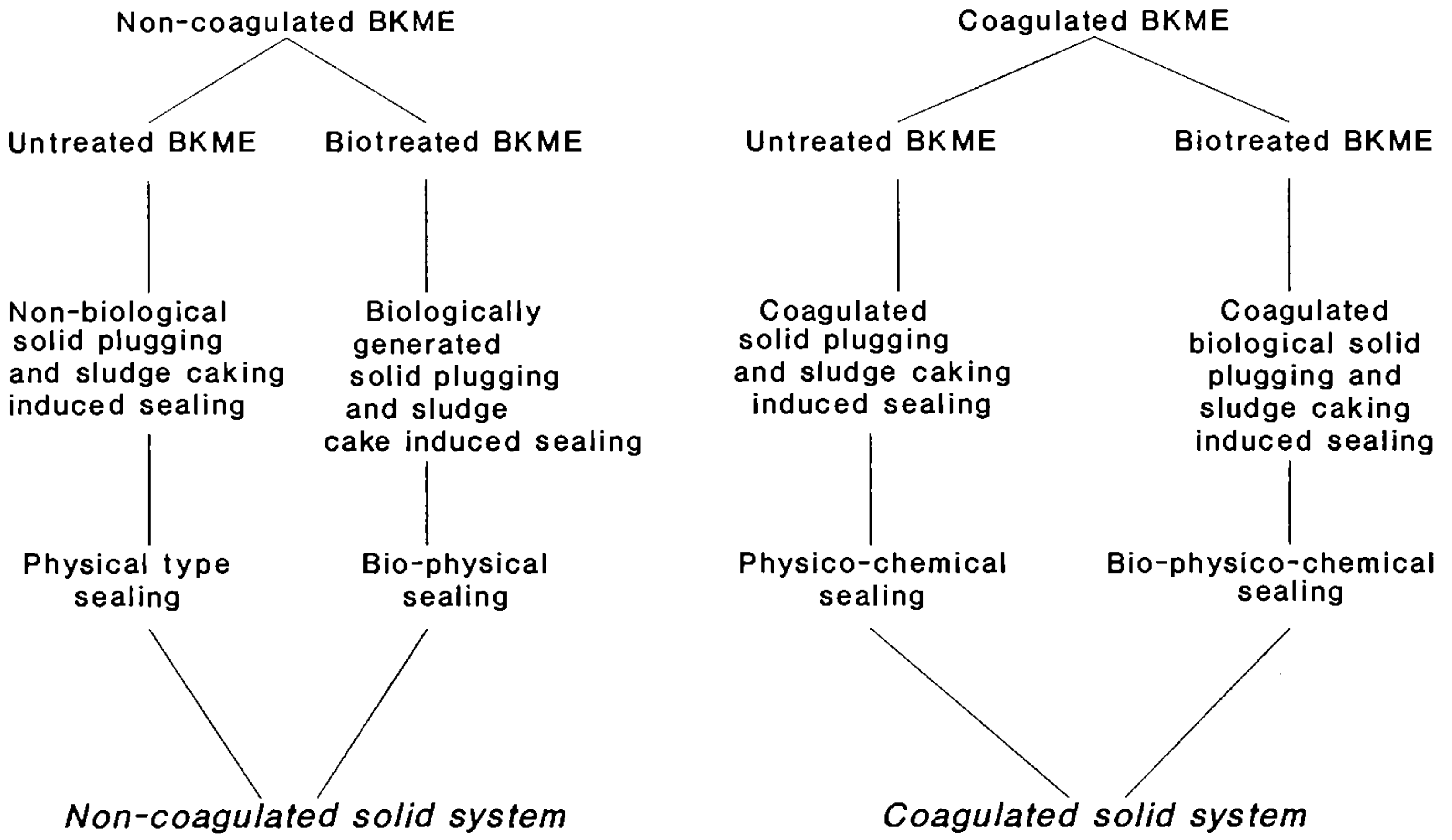

Note: Physico-chemical type of sealing can also be obtained via interaction of fluid phase with basin soil material through induced swelling.

Fig. 1 -- Types of Sealing

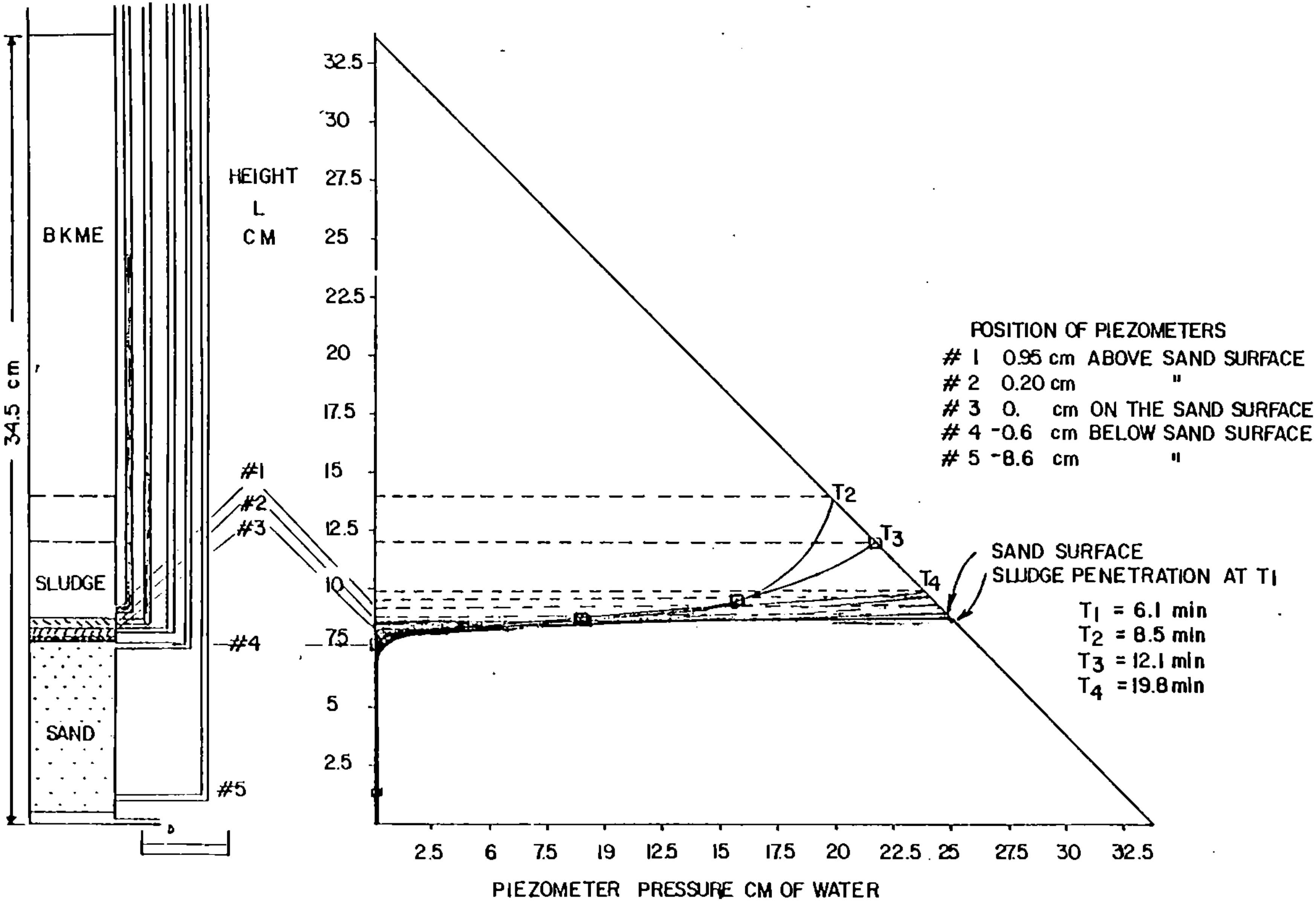

Fig. 2 -- Settling Column and Piezometric Pressures

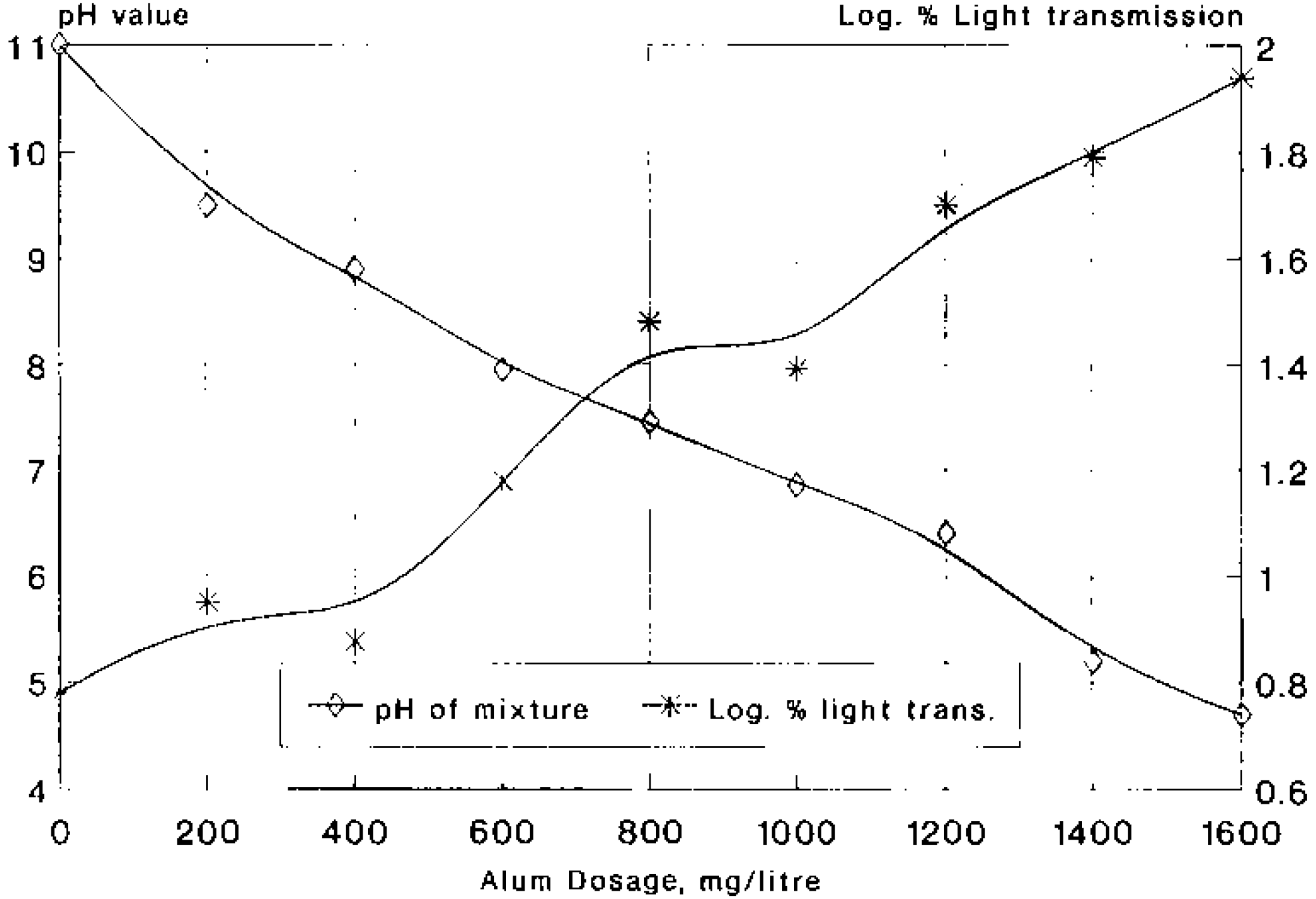

Fig. 3 -- Settling of Alum-BKME

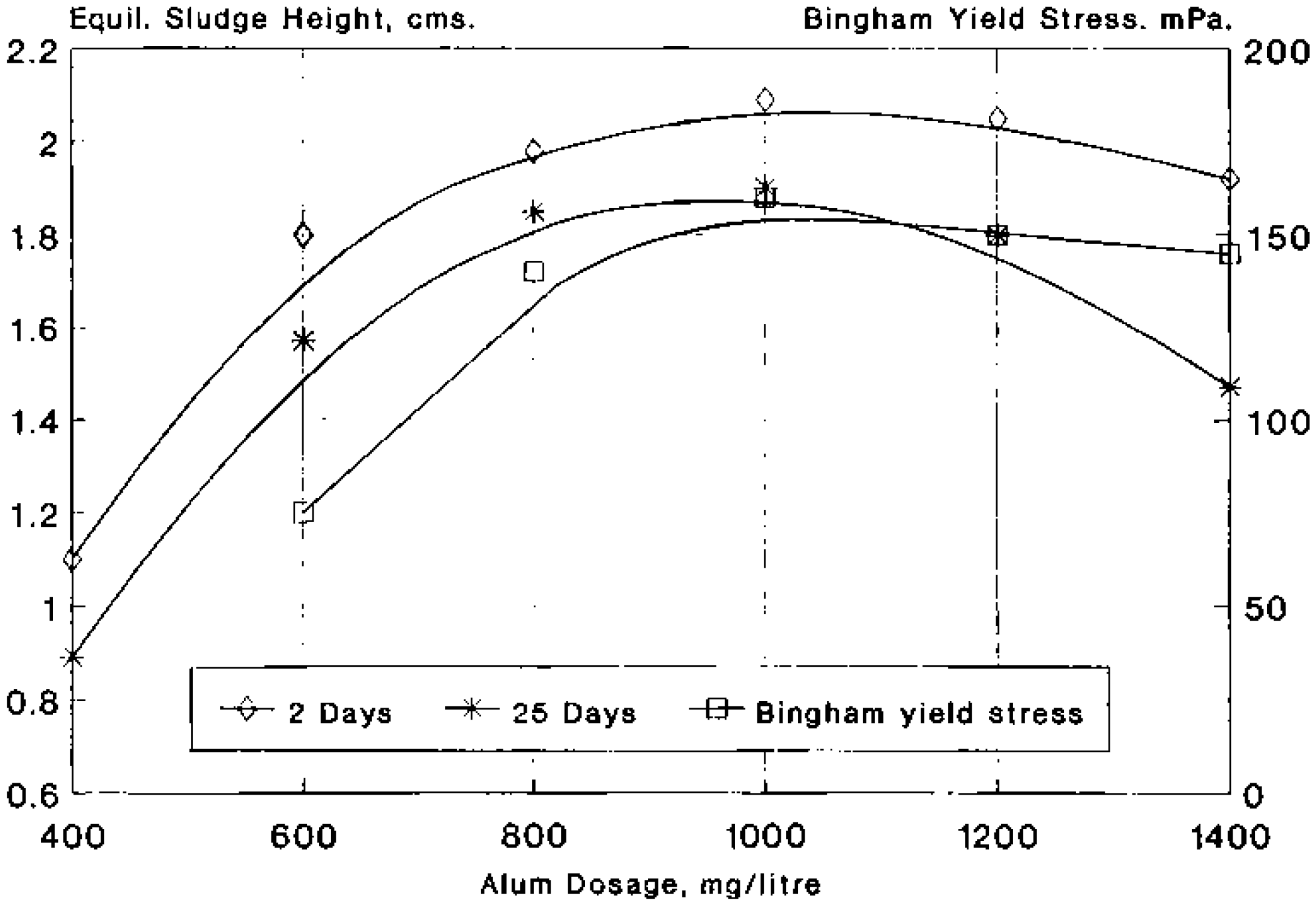

Fig. 4 -- Equilibrium Sludge Height

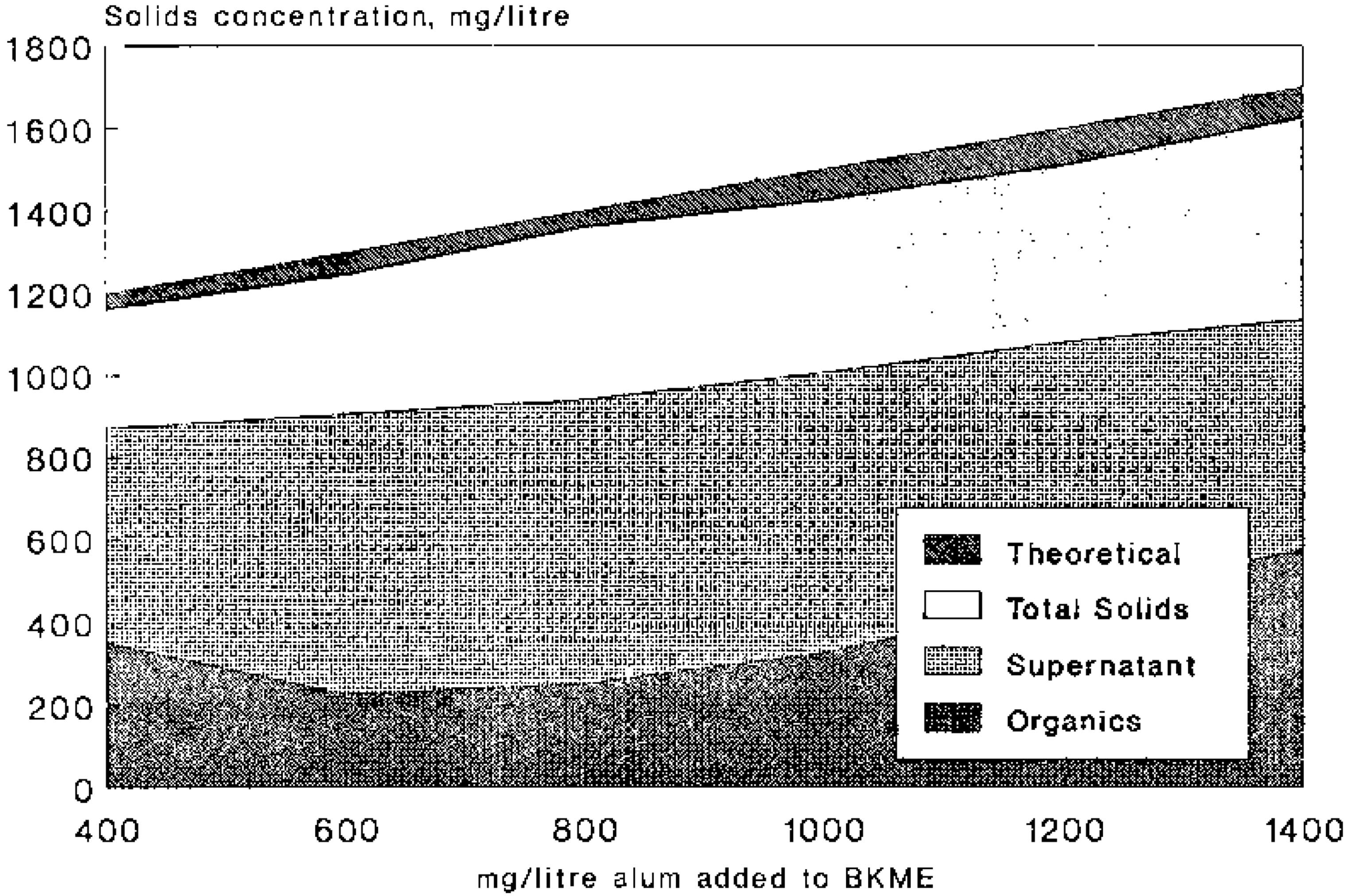

Fig. 5 -- Total Solids Mass Balance

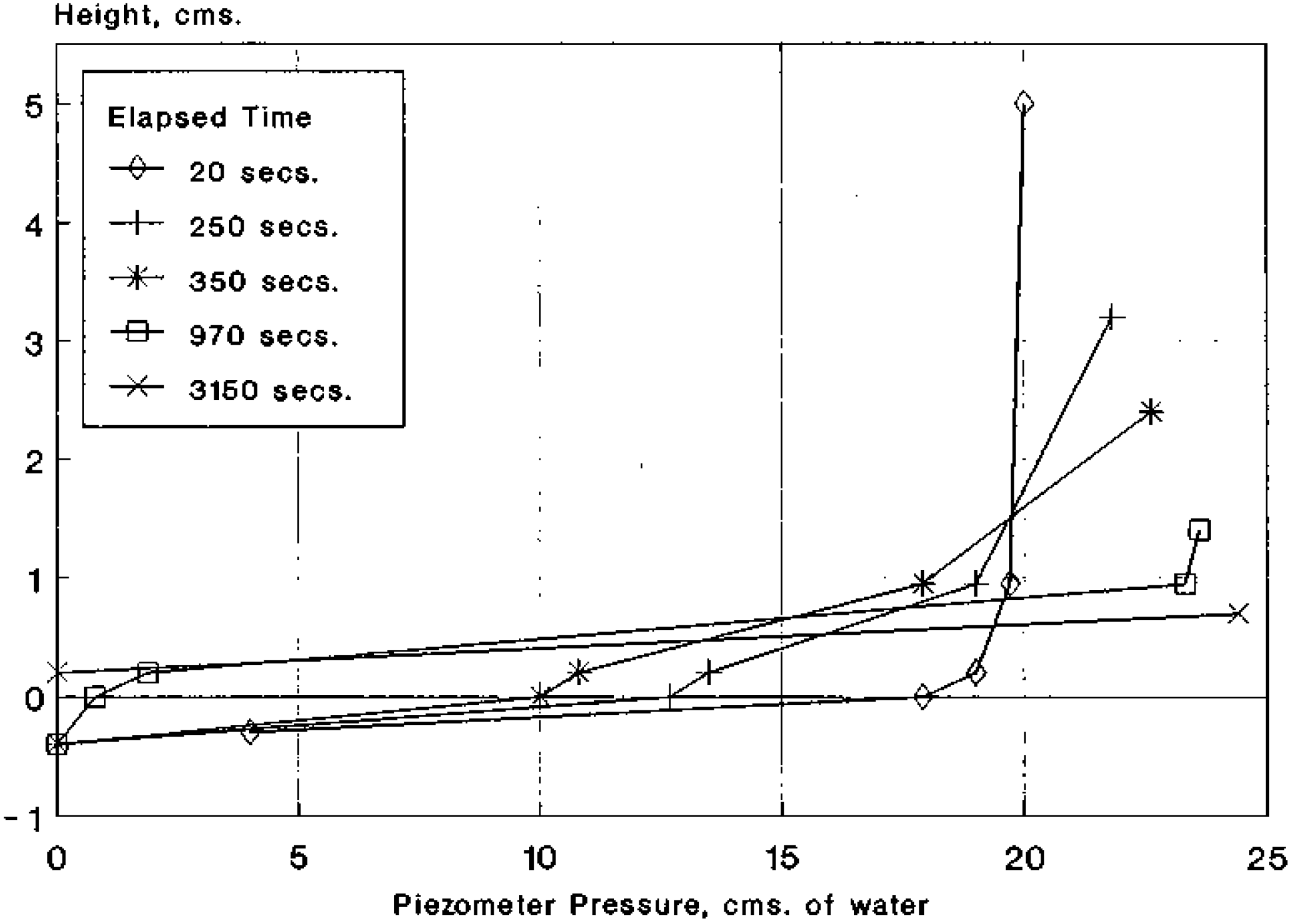

Fig. 6 -- Development of Sludge Cake

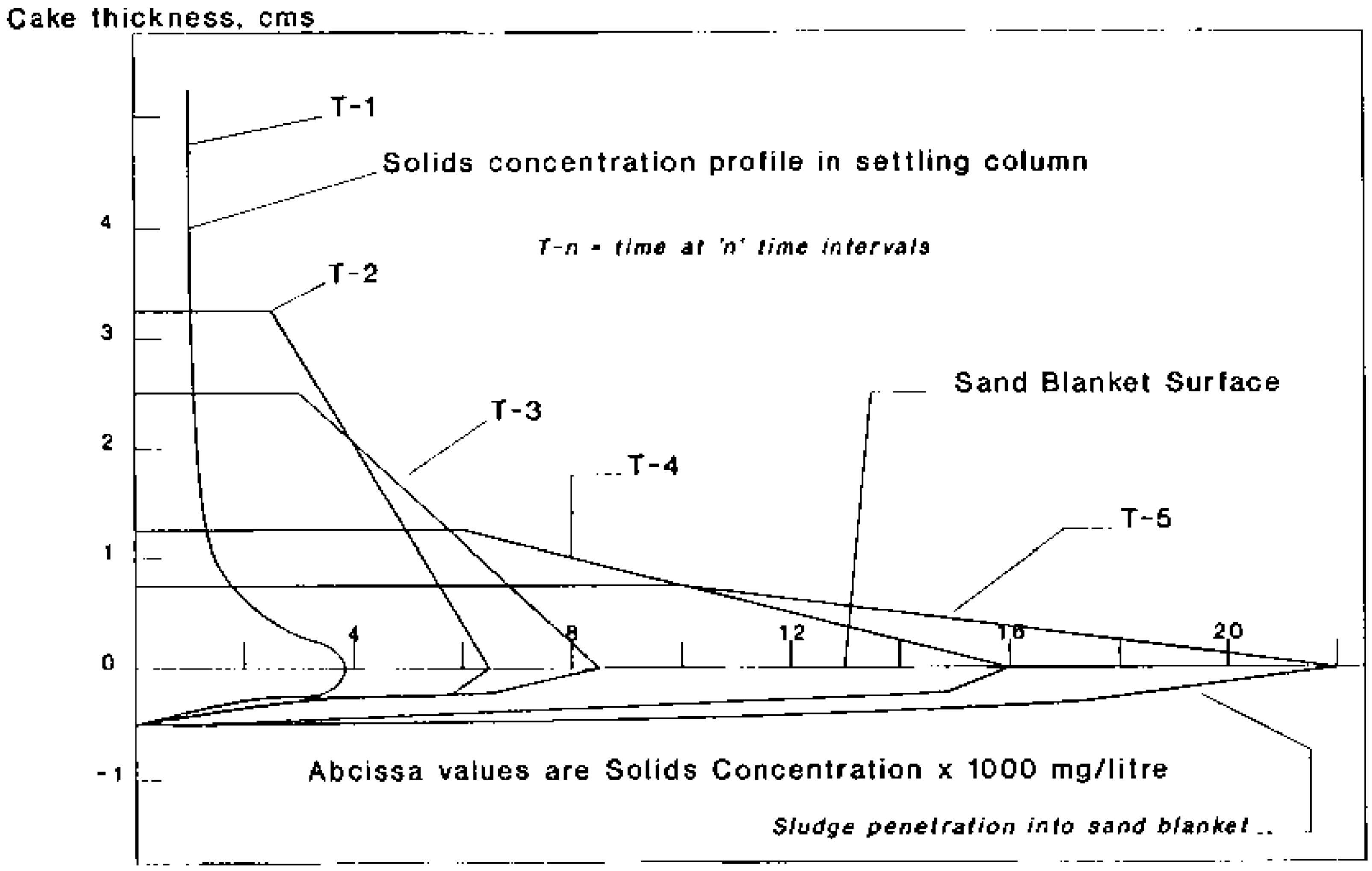

Fig. 7 -- Assumed Solids Concentration Profile

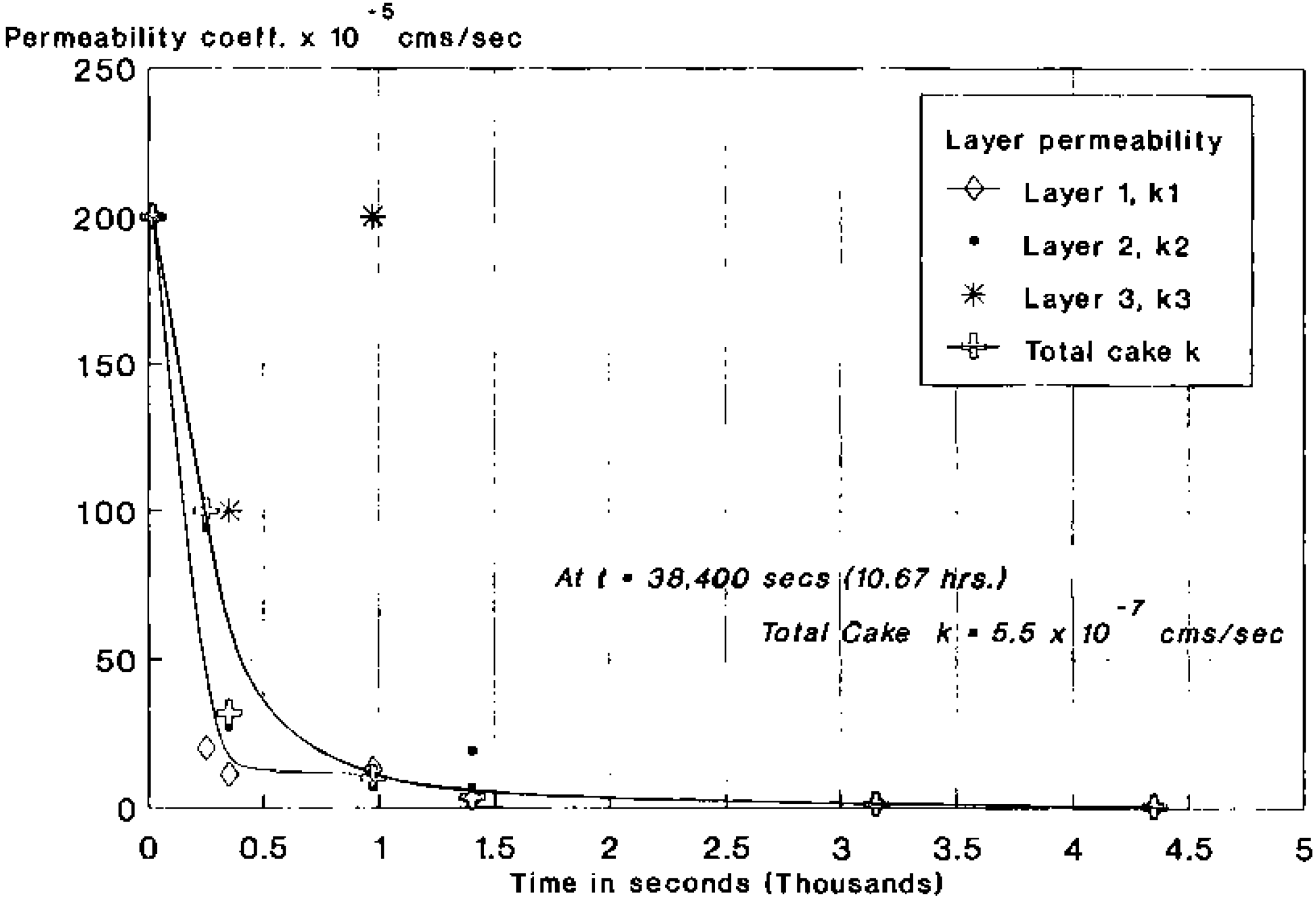

Fig. 8 -- Coefficients of Permeability

GROUNDWATER CONTAMINATION BY INDUSTRIAL AND DOMESTIC WASTES: A CASE STUDY

BY

RAYMOND N. YONG[1] AND MOSTAFA A. WARITH[2]

INTRODUCTION

Within the framework of the evaluation program of waste disposal sites on federal land in Quebec, the Patton Landfill site in Kahnawake, has held the attention of the Environmental Protection Service of Canada for the purpose of carrying out a detailed hydrogeological and geochemical study. The main purpose of the present investigation is to continue the work already in progress since 1984, for analyzing the underground water in the immediate vicinity of the Patton Landfill, and to evaluate the potential impact of the presence of priority pollutants on the environment and on public health.

The Patton Landfill is located on the heart of the Kahnawake Indian Reservation, to the south of the island of Montreal. The site, which has been in full operation from 1964 until 1986, received 2.9 million cubic metres of various types of organic and inorganic industrial and domestic wastes. This amount of waste has been landfilled on a site covering 46 hectares. According to the

---

[1] William Scott Professor of Civil Engineering and Applied Mechanics, and Director of the Geotechnical Research Centre, McGill University, Montreal, Quebec.

[2] Project Coordinator, Conestoga-Rovers & Associates, Waterloo, Ontario.

Environmental Protection Service (EPS) recommendations, the site now only accepts dry materials, mainly demolition waste, to be used as a final cover for the previously landfilled waste. Figure 1 depicts the area which land filling has been taking place, in addition to the various monitoring wells which are available for periodical sampling.

The wastes were placed over glacial deposits of fine silt and heterogeneous till to an average thickness of 16 metres. Between the till and limestone bedrock, a layer of one to two metres of fluvio-glacial sands is found. This deposit forms a good aquifer that is yielding groundwater to the domestic wells in the area. Figure 2 displays a cross-section soil profile at the landfill site.

It was shown by the previous hydrogeological studies that:

(1) the pheratic water present in the waste on top of the glacial deposits flow radially, and discharges into the surrounding marshes and the Little Suzan River.

(2) the flow in the underlying aquifer is directed towards the south-east, in the Big Suzan River basin,

(3) the flow is redirected to the north-east in the direction of the St. Lawrence Seaway, and

(4) the advective flow pattern between the phreatic water and the aquifer is essentially downward.

These observations highlighted the potential hazard of the Patton Landfill Site and the need for regular monitoring to determine the aerial extention of contaminants migrated to the subsurface environment.

METHODOLOGY

The sampling of the Patton Site by the Geotechnical Research Centre of McGill University was carried out in September, 1987. Several groundwater samples were collected from the multilevel monitoring wells, installed previously by both Amentech Inc. (1984) and Foratek International Inc. (1986), using teflon bailer with a capacity of 2 litres. In some of the wells, due to the distortion of these wells and the inability of the bailer to pass through the wells, a peristaltic suction pump with a disposal tygon tubing was used. The monitoring wells were 50 mm in diameter with depth varying from 3.50 to 40.0 metres. The wells are divided into four groups namely: A, B, C and D, is the deepest (Table 1).

To avoid cross-contamination, before each sample was taken, the bailer was washed with deionized water. This was followed by acetone treatment and a final rinse with deionized water. The collected samples were contained in glass opague bottles to minimize photodegradation and biochemical/chemical changes during the time taken to transport and store the samples in the laboratory.

The samples were analyzed at the field for the following parameters: pH, conductivity, redox potential, and temperature. In addition, the water level at each well was recorded.

Laboratory chemical analyses were conducted to determine the presence of heavy metals, major cations, major anions, as well as the organic load measured as total organic carbon (TOC). Furthermore, the water samples were submitted for the analyses of specific trace organics, such as moncyclic aromatic hydrocarbons (benzene), PAHs, PCBs, and phenols. All the chemical analysis in this study followed the standard procedures described by the Environmental Protection Service, Laboratory Manual (1979).

The contours presented in this paper are obtained by bivariate linear interpolation of an estimated concentration grid followed by Bessel function smoothing and implemented in the Plot Call Computer Program Package (QGRID 87 and TOPO 87). Isocontours are generated for the purpose of establishing the direction and radial extent of the contaminant plum.

The Behaviour of Different Contaminant Species in the Landfill Area

The groundwater quality is affected by numerous parameters including heavy metals, phenols, monocyclic aromatic hydrocarbons (benzene), PAHs and PCBs. The results of the analyses of the samples collected in September 1987 are presented in Tables 2, 3, 4, 5 and 6.

The water samples collected from the monitoring wells located directly in the fill zone itself (Well Nos. P-5, P-7, P-8 and P-9) were very mineralized, very hard, slightly charged with organic matter and contaminated with heterotrophic areobic and optional anaerobic bacteria. However, samples from wells at the periphery of the fill zone (Well Nos. PZ-2, P-12 and P-13) were less mineralized and charged with organic matter.

1. Changes in pH values

The pH values in the majority of the wells lies in the relatively narrow pH range of 6.5 - 8.0 (on average). These pH results provided in Table 2 indicated that the B type monitoring wells (located in the fine silt till layer) exhibited slightly higher pH values than the A type wells (located in the waste zone itself). The difference was on average in the order of 0.5 pH units. The pH values in the B and C type wells were approximately equal to pH 7.0; however, in A wells it was slightly acidic. These changes in the pH therefore reflects that: (1) the dissolved inorganic carbon exists almost entirely as

HCO_3, and (2) the subsurface soil has buffering capability. The alkalinity, HCO_3, and CO_3, results corroborated the above-mentioned observation (Tables 2 and 4).

2. Redox Potential

The redox conditions within the landfill were sufficiently reducing in nature, the in-situ measured values of redox potential were in the negative side of the redox scale with an average value of -260 mV. Generally, the landfill becomes predominately anaeorbic shortly after emplacement. The conditions are relatively anaerobic in the proximity of the surface of the refuse area and become increasingly anaerobic towards the bottom. These conditions, in turn, may prevent the formation of SO_4 and/or NO_3 from any sulphur or nitrogen compounds possibly present in the waste. These reduction reactions generate CO_2. Table 2 summarizes the results of redox potential (Eh) and the partial pressure of carbon dioxide (PCO_2). The results of PCO_2 are back-calculated from the chemical measurements and the computer program WATEQ (Trusdell and Jones, 1974). The partial pressures of CO_2 at A level wells are in the range of 10^{-3} to 10^{-2} bar, which is typical for these types of environmental conditions (Freeze and Cherry, 1979). These values of PCO_2 were considerably higher than the PCO_2 of the earth atmosphere ($10^{-3.5}$ bar). It is pertinent to note that PCO_2 in the A type wells are higher than those in the B wells by almost one order of magnitude. This is due to the microbial activity taking place in the refuse layers.

Similarily, high values of PCO_2 were observed in the samples collected at Well Nos. P-5C, P-9C and P-11C. This indicates that the groundwater at C type wells in the Patton Site became charged with CO_2 during infiltration from the fill layer into the subsurface layers. The high CO_2 partial pressure emanated from the degradation of organic matter by different microorganisms operating in the subsurface environment.

3. Conductivity and Total Dissolved Solids

The conductivity values for the groundwater samples indicate a substantially high salt content in all Well levels A, B and C. These results are consistent with the measured total dissolved solids (TDS). By and large, there is a perceptible difference in TDS concentrations in the A and B wells. The TDS concentrations in the A level are in the range of 1000 - 4000 mg/L with an average value of 2030 mg/L. On the other hand, at the B level wells, TDS concentrations are in the range of 400 - 800 mg/L with an average value of 570 mg/L (Table 2). These results indicate the effect of the filtration and microscreening action provided by the soil medium underneath the landfilled waste. Ionic strength results back-calculated from WATEQ computer program are presented in Table 2. Figure 3 displays the extent of TDS at level B. The TDS contours suggest that contamination plum is migrating south east. This corresponds to the approximate direction of groundwater flow in the Patton Landfill Site.

The high TDS concentration at level C is found to be mainly due to the dissolution of calcite ($CaCO_3$)and dolomite ($CaMg(CO_3)_2$). Table 3 provides the concentration of Ca and Mg in the different wells, the average Ca/Mg molar ratio is greater than unity, which clearly indicates that the calcite is dissolved more rapidly than dolomite in the aquifer level. This observation can be attributed to the fact that the infiltration of rain water and snowmelt into the subsurface soil became charged with CO_2 and moved into the soil zone that contains both calcite and dolomite. This is what probably caused the dissolution of both minerals. Table 3 also shows that calcite dissolves much more rapidly than dolomite and that saturation by calcite is attained before that of dolomite.

4. Heavy Metals

The amounts of heavy metals cadmium and lead found at Well Nos. P-5, P-7 and P-8 were high in relation to the quality criteria for drinking-water. However, the other heavy metals such as zinc, copper, and iron did not occur at levels above the drinking-water limits (MENVIQ 1983). From the consideration of solubility and observed pH values in levels B and C, it is expected that solid-phase solubility should severely limit the appearance of most heavy metals and selectivity coefficient constraints, its also expected that absorption would be a crucial mechanism in limiting the mobility of some of these metals (Yong et al., 1986). These observations are supported by the fact that, a fairly important drop in copper and zinc concentrations occurred, between December, 1984 and September 1987.

The concentration of mercury in the aquifer level (level C) was found to be higher than the maximum permissible limits for drinking-water (2 µg/L) (MLAE, 1983). The concentration of mercury in the waste layer was above this limit with an average value of 150 µg/L. The highest concentrations were found at Well Nos. P-7A and P-8A (Table 4). The average concentration of mercury in the B level (till layer) was in the range of 6 µg/L.

Cyanides was detected in the waste at moderate concentrations at Well Nos. P-5A and P-7A. However, at Well No. P-9A, the cyanides concentration was found to be extremely high, in the range of 1500 µg/L, which is way above the limits for drinking-water of 200 µg/L (Table 4). The migration of cyanides from the fill zone to the subsurface zone was evident, because the concentration of cyanides at P-9B and P-9C was 473 and 79, respectively.

5. Chloride and Other Anions

The behaviour of chloride ions was studied mainly to separate the effect of dispersion and chemical processes operating in the subsurface environment at the landfill. The chloride attentuation was relatively low (Table 4). The chloride concentrations at A level wells measured in September, 1987 were found to be higher than those values previously obtained in 1985 and 1986. The increase in chloride concentration ranged between 90 - 400 mg/L (e.g. Well Nos. P-5A, P-7A and P-8A). The chloride concentration in B type wells were relatively lower in comparison with the drinking-water standard (MENVIQ, 1983). However, only in Well No. P-7B, the chloride concentration was found to be relatively high. This observation may suggest a direct contact between the landfilled waste and the groundwater through a more permeable soil strata in this location. Chloride levels on the aquifer are detected in relatively high concentrations, especially in Well Nos. P-5C and P-12C. This could indicate the presence of NaCl that leached from the sediments.

The three other anions examined during the course of this study were CO_3, HCO_3, and SO_4 (Table 4). It was observed that the concentrations of CO_3 are generally very low. There are tow phenomenon which can contribute to these findings: (1) the redox conditions within the landfill zone, and (2) the pH range of the groundwater was in the narrow range of 6.5 to 8, and this usually favours the formation of HCO_3 compounds rather than CO_3. HCO_3 is the dominating anion and SO_4 the second most abundant anion. The average HCO_3 value at the different sampling points is 548 mg/L. In some cases, the HCO_3 content in A type wells is more than twice as much as in B type wells.

A comparison between SO_4 content of the A and B wells show that the SO_4 content at the A wells in significantly higher than that at the B wells (e.g. Wells P-5, P-7 and P-9). In spite of the redox potential conditions within the fill area, the SO_4 concentration was found to be high with an average value of 90 mg/L. Figures 4 and 5 display the horizontal extent of HCO_3 and SO_4 in level A.

6. Migration of Organic Compounds

The Chemical Oxygen Demand (COD) measured in the vicinity of the landfill area in September, 1987 was found to be relatively low in comparison to the values measured previously in 1986. This was particularly true in the measurements taken at P-8A and P-9A Wells. The values of COD in those two wells were reduced from 262 to 97 mg/L and from 7560 to 80 mg/L for the Well Nos. P-8A and P-9A, respectively. It is pertinent to note that the COD level was above the permissible limits of drinking-water (MENVIQ, 1983).

Table 5 provides the results of the COD and the total organic carbon (TOC) measured in the different monitoring wells. These two parameters (COD and TOC) indicate the amount of organic content present in the water samples. The organic compounds measured consist of biologically degradable compounds which remain in solution, principally fluvic acid, in addition to a variety of other synthetic organic contaminants. Such organic compounds were found to be highly mobile in a soil-water system and could present a vertibale threat to groundwater quality even in miniscule concentration.

The total organic halogen (TOX) as an indication of the synthetic chemical contamination was also measured. It was found that TOX concentrations in Well Nos. P-5A, P-7A, P-8A and P-9A were above the maximum limits of drinking-water (10 µg/L). The average concentration of TOX in the A level (waste zone) is estimated to be in the order of 18 μg/L, which expresses the total concentration of PCBs, pesticides, and any other chlorohydrocarbons compounds present in the landfilled waste. As noticed in **Table 5**, no TOX were detected in the B and C levels except at Well Nos. P-9C and P-10B.

There is ample evidence that organic trace contaminants interact with soil solids and microorganisms during leachate movement into the subsurface environment. Sorption retards solute transport, whereas both sorption and dispersion attenuate leachate organic concentration. The long solute residence time, owing to sorption coupled with low hydraulic velocities, together with high specific surface area of the porous medium, affords perfect opportunities for microbial growth and biodegradation.

7. PCBs and Other Priority Pollutants

The presence of PCBs (aroclor 1260 especially) in very high concentrations in comparison to the criteria for drinking-water in the vicinity of the landfill (level A, e.g. Wells P-5, P-7, P-8 and P-9) were detected in the samples collected since December, 1984. In Well Nos. P-5A and P-7A, the PCB concentrations were above 1 μg/L (Table 6). Figure 6 displays the spreading of PCB plume under the Patton Site. In the preliminary study of December, 1984 and June, 1985 PCBs (aroclor 1242, 1254) and four organochloride pesticides were detected at the Little Suzan River which is located at the south-east perimeter of the Patton Landfill Site. The PCBs concentration of 0.2 mg/kg soil was detected in the river sediments. Our follow up of the river sediment analyses will be reported in subsequent stages.

Phtalate ester compounds were detected in relatively high concentrations in the forms of di-n-butyl phtalate di (2-ethylhexyl) phtalate. These phtalates are present in the waste from many different sources because of its use as a common agent in plasticizrs, insecticides, ink prints and paints. The concentration of total phtalate at P-9A exceeded 6300 µg/L, however, at P-8A the concentration was found to be 80 µg/L (the maximum permissible limits is 50 µg/L) (Table 6). The phtalate compounds were also found in level B and C wells.

Many monocyclic and the polycyclic aromatic hydrocarbons such as: benzene, toluene, xylene, chlorobenezen, etc. (Table 6), were detected in fairly high concentration in level A wells. The polycyclic aromatic hydrocarbons (PAHs) were found in the waste in both solid and liquid forms (Environment Canada, 1986). PAHs are relatively insoluble in water with solubilities of about 10^{-10} M, however, they could be synthesized by microorganisms, algae and plants.

The results of the phenol or hydroxybenzene (C_6H_5-OH) measurements are provided in Table 5. It can be concluded that phenols is one of the most crucial contaminants in the Patton Landfill Site. Phenol concentrations found in the A wells are in the range of 16 to 40 µg/L with an average value of 25 µg/L. On the other hand, phenols concentration were detected in B Wells, with concentrations ranging from 12.5 to 23 µg/L with an average value of 15.6 µg/L. These results suggest that the phenols migrate from the fill zone to the subsurface zone, where the phenols were detected in fewer concentrations (Figure 7). In addition, phenols were detected in the wells on the periphery of the fill zone (Well No. P-13) and in some leachate samples collected from a spring 200 metres east of Well P-5.

SUMMARY

This study made it possible to substantiate the presence of a potentially serious impact of public health and on the environment and the need for regular monitoring. The migration and the extention of contaminant species were found to be limited to the landfill vicinity: however, the following suggestions were made to avoid pollution progression:

(1) Current landfilling of dry material should be avoided to limit the amount of leachate production.

(2) The landfill site should be covered with soil of low permeability to reduce the infiltration rate of water from rain and melted snow.

(3) Ditches should be dug around the vicinity of the fill zone in order to collect the runoff. The marshes at the west end of the site should be drained. In addition, ditches are vital to intercept the drainage water from the Caughnwawga Golf Club, which is located on the north side of the Patton Landfill.

(4) Monitoring the groundwater and surface water quality on both the landfill zone and the south-east downstream zone is recommended to determine if water treatment is necessary. This will require an effort to increase the number of monitoring wells at different levels. This is especially true since some of the existing monitoring wells are not functioning properly (e.g. PZ1, PZ3, PP1, PP2 and P-10).

(5) In-situ biodegration of the organic content should be considered as an option to reduce the highly toxic organic compounds detected in the fill zone.

ACKNOWLEDGEMENTS

The authors wish to acknowledge the valuable discussion and information provided by Mr. Gerald Girouard and Richard St. Germain of Environment Canada, Quebec Region. The cooperation of Dwain White of Mohawk Council of Kahnawake in the conduct of this study is also gratefully acknowledged.

REFERENCES

Environment Protection Service (1979). "Laboratory Manual", Government of Canada, Department of Environment.

Environment Canada (1986). "Etude Hydrogeologique Du Site De Disposition De Dechets No. 06-01-05 Patton", Report No. 768 146 p.

Freeze, R.A. and Cherry, J.A. (1979). "Groundwater", Prentice-Hall, Inc. London, 604 p.

Ministere Du Logement De l'Amenagement Et De l'Environnement des Pay-Bas (1985). "Loi Interimiare su la Deposition des Sols", Constat de l'Importance de la contamination d'un sol au Pay-Bas.

Ministere De l'Environnement Du Quebec (1983). "Reglement sur les Dechets Solides". Loi sur la qualite de l'Environnement. Decret 194-82.

Nyer, E.K. (1988). "Treatment of BTXE compounds at Low Flow Rate". Groundwater, Monitoring Review, Spring 1988, pp. 42-46.

Trusdell, A.H. and Jones, B.F. (1974). "WATEQ, A Computer Program For Calculating Chemical Equilibria of Natural Waters," J. Research V.S. Geolol. Survey, Vol. 2, No. 2, pp. 233-248.

Yong, R.N., Warith, M.A. and Boonsinsuk, P. (1986). "Migration of Leachate Solution through Clay Liner and Substrate" Hazardous and Industrial Solid Waste Testing and Disposal, ASTM-STP 933 pp. 208-225.

TABLE 1

LOCATION OF MONITORING WELL SYSTEMS

			Level (m)			
Monitoring Well	X(m)[1]	Y(m)	A[3]	B[4]	C[5]	D[6]
P-2	642	486	—	—	—	42.0
P-5	575	390	6.92	23.04	28.72	—
P-7	494	345	5.0	15.38	31.31	39.92
P-8	325	675	7.72	12.68	25.37	—
P-9	300	0.0	8.0	18.70	29.43	000
P-10	200	228	3.90	20.47	—	—
P-11	0.00	208	—	12.67	24.76	—
P-12	158	653	—	7.05	15.20	—
P-13	992	176	—	12.38	18.61	—
PP1	767	411	—	—	—	21.57
PZ1[2]	517	340	—	—	—	
PZ3[2]	833	528	—	—	—	—
PZ4[2]	75	120	—	—	—	—

Note: 1 X and Y coordinates are measured in reference to horizantal and vertical axes passing through P-9 and P-11, respectively.
2 is non-existant (buried)
3 A located in the fill
4 B located in the silt clay
5 C located in the till rock interface
6 D located in the rock

Table 2

GROUNDWATER PHYSICAL CHARACTERISTICS

Monitoring Well No.	pH	Conductivity meq/L	Ionic Strength x10^{-3}(1)	Redox Potential m V	Alkalinity $CaCO_3$ (mg/L)	PCO2 (bar) (1)	TDS mg/L
P2	9.1	3.58	8.72	-256	111	8.72×10^{-3}	744
P-5A	6.7	18.67	23.90	-266	235	2.39×10^{-2}	989
P-5B	7.2	6.54	14.40	-247	324	1.44×10^{-2}	586
P-5C	6.4	28.60	53.90	-270	697	5.39×10^{-2}	2360
P-7A	6.5	23.20	27.80	-281	936	2.78×10^{-2}	1860
P-7B	7.0	24.90	46.40	-263	1192	4.64×10^{-2}	2103
P-8A	6.7	20.90	4.30	-297	608	4.30×10^{-2}	1712
P-8B	7.8	4.90	7.77	-287	330	7.77×10^{-3}	385
P-9A	6.6	43.80	54.20	-270	2111	5.42×10^{-2}	3974
P-9B	8.3	3.80	7.73	-258	273	7.73×10^{-3}	3959
P-9C	8.0	4.10	9.94	-267	269	9.94×10^{-3}	408
P-11B	7.0	12.20	16.20	ND(2)	318	1.62×10^{-2}	779
P-11C	7.7	155.00	11.00	ND	390	1.10×10^{-2}	707
P-12B	7.0	436.00	33.60	ND	ND	3.36×10^{-2}	1617
P-12C	7.0	1.95	16.00	ND	450	1.60×10^{-2}	700
P-13B	7.6	4.50	10.40	ND	282	1.04×10^{-2}	450
P-13C	8.5	8.90	10.60	-262	648	1.06×10^{-2}	737

(1) Data back-calculated from WATEQ Computer Program (Trusdell and Jones, 1974)

(2) ND = not detected

Table 3

MAJOR CATION CONCENTRATIONS

Monitoring Well No.	Ca	Mg	Na	K	Saturation Index (Si) Calciate $CaCO_3$	Saturation Index (Si) Dolomite $CaMg(CO_3)_2$	Mole Ratio Ca/Mg
P2	12.3	6.7	76	7.2	–	–	–
P-5A	181.1	64.6	196	89.0	–	–	–
P-5B	184.6	21.4	32	5.2	–	–	–
P-5C	664.3	73.5	209	18.5	-0.843	-0.032	5.50
P-7A	31.8	123	256.6	9.4	–	–	–
P-7B	397.7	119	347	5.2	–	–	–
P-8A	416	152	105	11	–	–	–
P-8B	56	21	38	8.2	–	–	–
P-9A	141.8	120.6	445	288	–	–	–
P-9B	71	5.6	33	6.3	–	–	–
P-9C	127.8	13.4	6.5	2.9	0.485	06.44	5.70
P-11B	167.3	13.4	12.2	2.0	–	–	–
P-11C	27.4	6.2	155	5.9	-2.437	0.951	2.68
P-12B	137.9	42.7	436	172	–	–	–
P-12C	201	18.9	0.9	5.7	0.40	0.652	6.40
P-13B	11.7	5.2	7.2	4.1	–	–	–
P-13C	156.7	1.3	192	6.1	0.385	-0.034	5.3
Permissible* limits for drinking water	200	150	270	–	–	–	–

* (MLAE, pays Bas, 1983)

** All units in mg/l

Table 4

ANIONS AND HEAVY METAL CONCENTRATIONS

Monitoring Well No.	Cl (mg/L)	SO_4 (mg/L)	HCO_3 (mg/L)	CO_3 (mg/L)	Pb (mg/L)	Zn (mg/L)	Cd (mg/L)	Cr (mg/L)	Hg (μg/L)	CN (μg/L)	Cu (mg/L)
P-2	7.1	1.3	634	0.9	0.3	ND**	ND	ND	ND	ND	ND
P-5A	163	96	--	2.5	0.2	ND	ND	ND	8.8	34	ND
P-5B	35.5	81.6	225.7	0.5	0.2	ND	ND	ND	7.0	368	ND
P-5C	490	148.8	736.4	1.1	1.1	ND	ND	ND	ND	109	ND
P-7A	227	158.4	969.9	4.1	1.0	ND	ND	ND	374.0	25	ND
P-7B	340.8	12.4	878.4	2.8	0.3	ND	ND	ND	0.8	98	ND
P-8A	349	24.5	634.4	--	ND	ND	ND	ND	314.0	9	ND
P-8B	7.1	47.5	207.4	0.7	ND	ND	ND	ND	1.7	298	ND
P-9A	369	749	1854.4	7.1	ND	ND	ND	ND	12.0	1550	ND
P-9B	28.4	86.4	164.7	7.1	ND	ND	ND	ND	ND	473	ND
P-9C	7.1	86.4	164.7	--	ND	ND	ND	ND	ND	79	ND
P-11B	70.9	249.6	250	--	ND	ND	ND	ND	21.0	111	ND
P-11C	21.7	192	299	--	ND	ND	ND	ND	0.8	14	ND
P-12B	709	120	835.7	--	ND	ND	ND	ND	11.0	4	ND
P-12C	141.8	45	286.7	--	ND	ND	ND	ND	0.7	825	ND
P-13B	7.1	62.4	207.4	0.4	ND	ND	ND	ND	ND	87	ND
P-13C	28.4	105.6	390.4	1.6	ND	ND	ND	ND	1.6	2	ND
Permissible* limits for drinking water	250	500	--	--	0.05	0.01	0.005	0.02	0.3	1.0	--

* (MLAE, Pay Bas, 1983)

** ND = not detected

Table 5

ORGANIC CONCENTRATIONS

Monitoring Well No.	COD (mg/L)	TOC (mg/L)	TOX (µg/L)	Phenols (µg/L)	Oil and Grease (mg/L)
P-2	26	ND**	ND	14	ND
P-5A	20	539	18.2	21	3.3
P-5B	–	ND	ND	12.5	0.9
P-5C	14	2.5	ND	12	ND
P-7A	24	86.5	23.7	25	1.2
P-7B	12	ND	ND	13	ND
P-8A	97	76.5	23.6	40	1.0
P-8B	13	ND	ND	23	0.90
P-9A	80	1560	17.1	16	3.6
P-9B	18	ND	ND	24	1.3
P-9C	22	31.5	6.1	15	1.8
P-11B	40	18.2	ND	19	ND
P-11C	4	ND	ND	18	ND
P-12B	ND	ND	ND	ND	ND
P-12C	104	44.3	ND	ND	ND
P-13B	ND	ND	ND	ND	1.2
P-13C	ND	ND	ND	11	0.9
Permissible* limits for drinking water	100	30	10	15	15

* (MLAE, Pay Bas, 1983)

** ND = not detected

Table 6

PRIORITY POLLUTANT CONCENTRATIONS

Monitoring Well No.	Benzene (μg/L)	Tolune (μg/L)	Xylenes (μg/L)	Elhyl-benzen (μg/L)	PCBs (μg/L)	Phtalate (μg/L)	Total PAH (μg/L)	BTXE (μg/L)
P-2	ND**	ND	ND	ND	ND	30.4	0.65	ND
P-5A	52.4	33.3	715	209	1.27	712.2	29.7	1009.7
P-5B	12	8	ND	ND	ND	ND	ND	20.0
P-5C	1.1	ND	ND	ND	ND	142.8	ND	1.1
P-7A	7.58	13.4	90	170	1.63	518	153.6	280.9
P-7B	68	20	28	ND	ND	ND	ND	90.8
P-8A	19.3	4.65	419	201	0.11	413.3	14	734.75
P-8B	16.7	ND	8.3	ND	ND	ND	ND	25
P-9A	30.4	1070	305	168	1.01	6361	48.2	1573.4
P-9B	16	36	8	8	ND	ND	ND	68.0
P-9C	6.4	2.7	ND	ND	ND	264.8	ND	9.1
P-11B	0.5	0.6	ND	ND	0.03	130.4	1.0	ND
P-11C	ND	ND	ND	ND	ND	ND	8.08	ND
P-12B	ND	ND	ND	ND	ND	ND	ND	ND
P-12C	11.7	ND	16.7	ND	ND	ND	94.1	28.4
P-13B	16	ND	ND	ND	ND	ND	ND	16
P-13C	ND	ND	ND	ND	ND	ND	ND	ND
permissible* limits for drinking water	–	–	–	–	0.2	50	10	450

* (MLAE, Pay Bas, 1983)

** ND = not detected

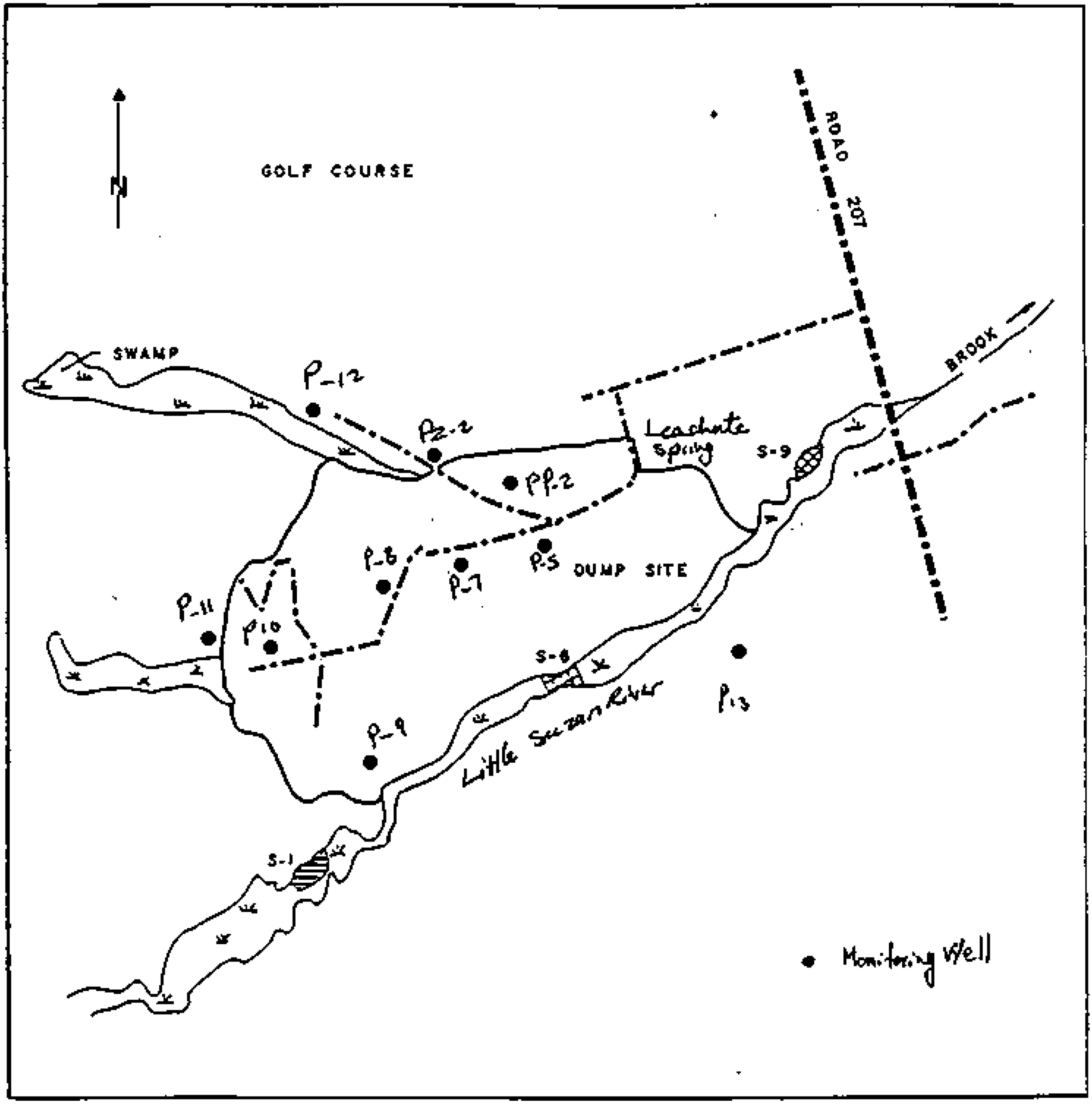

FIG. 1 General layout of the Patton landfill

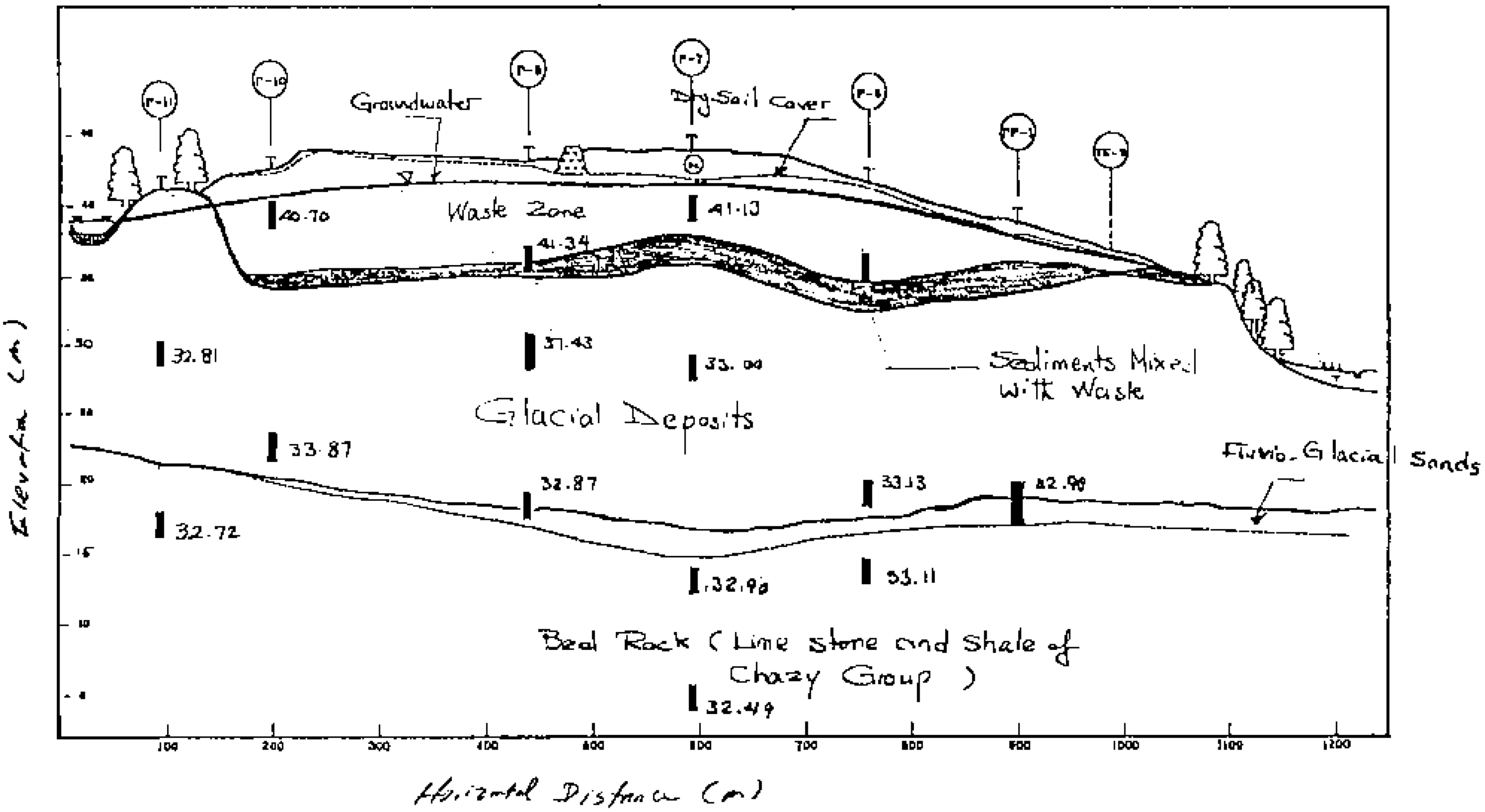

FIG. 2 Soil profile at Pattan landfill. (cross-section A-A)

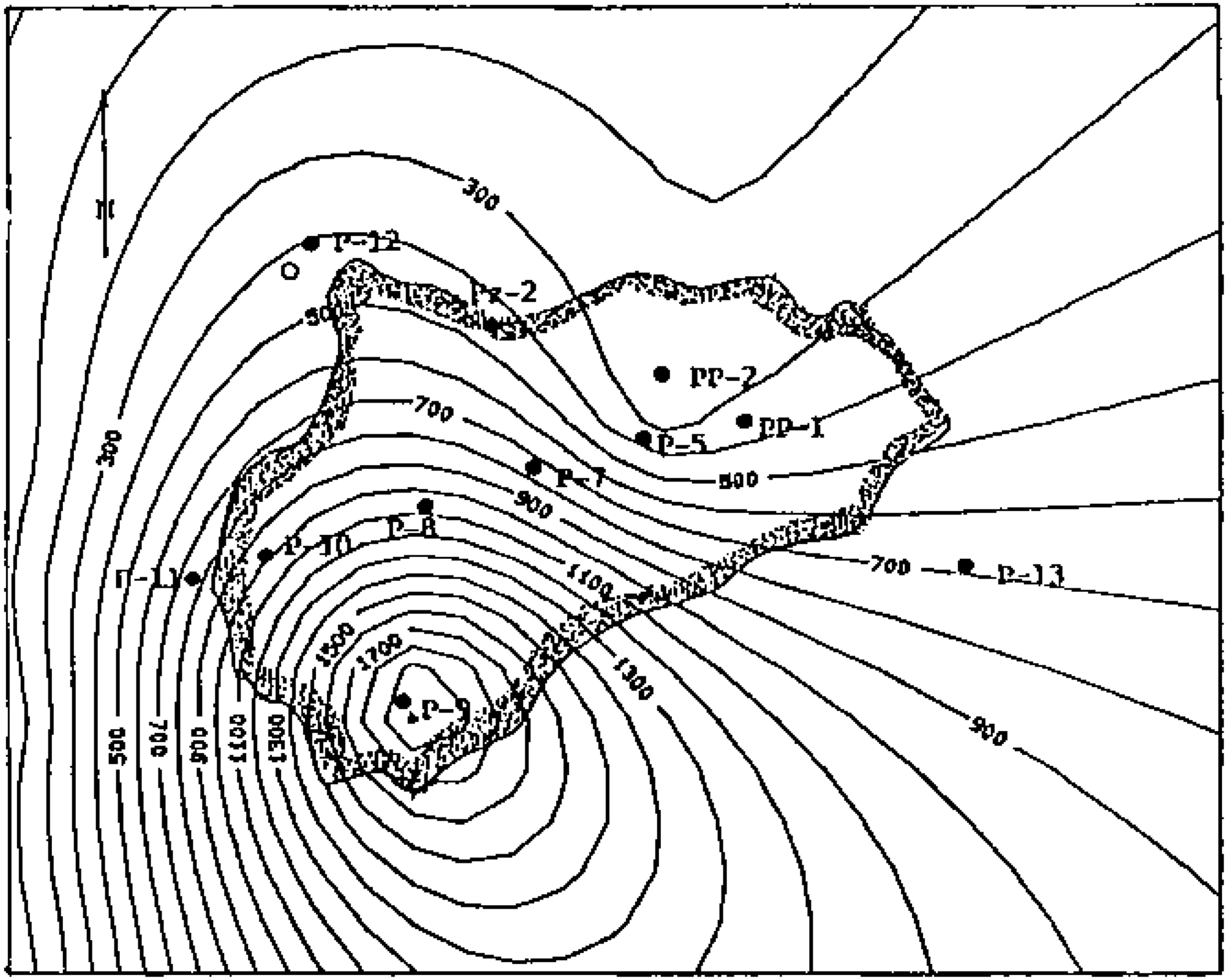

FIG. 3 Total dissolved solids (TDS) at level 0.

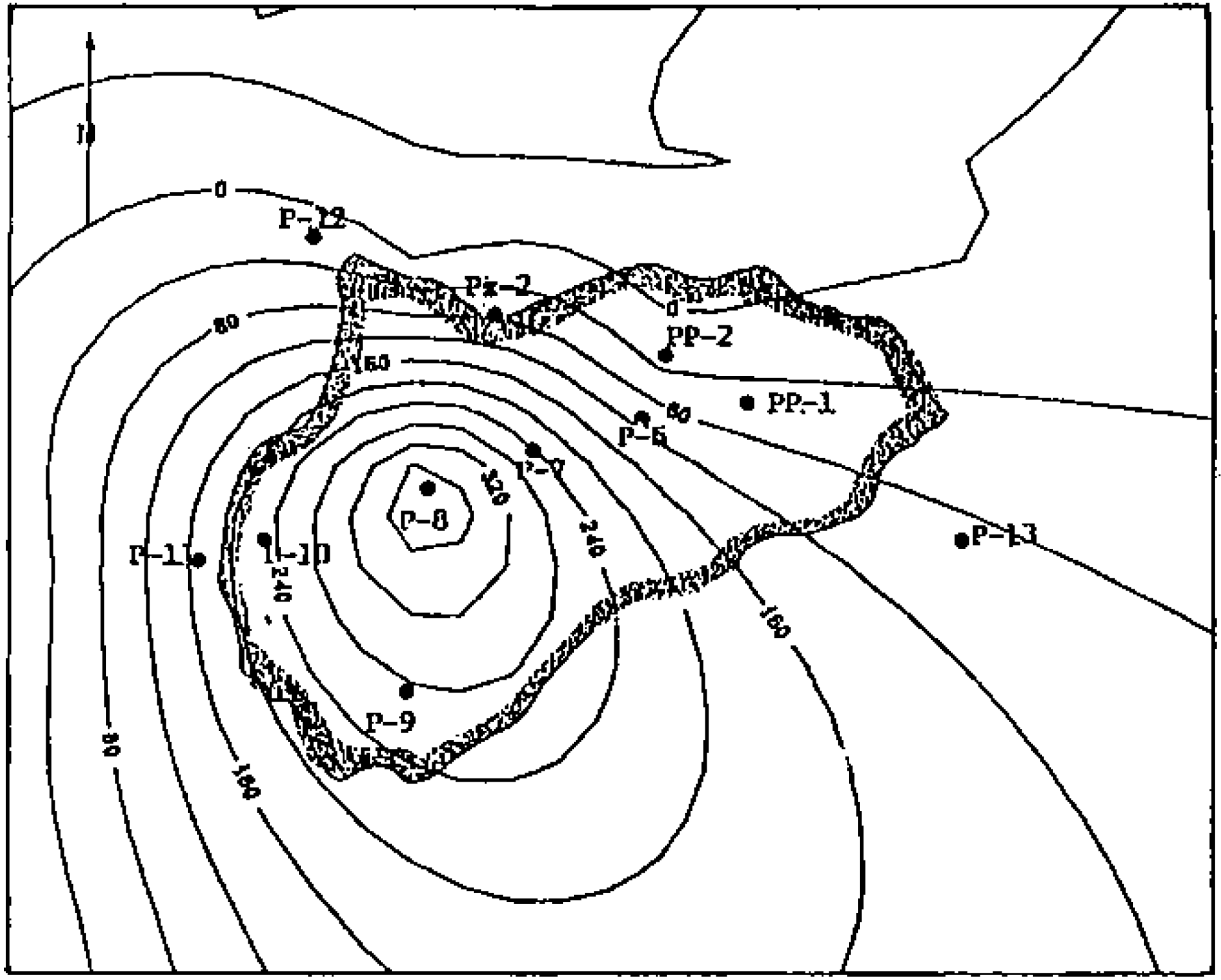

FIG. 4 HCO_3 at level A.

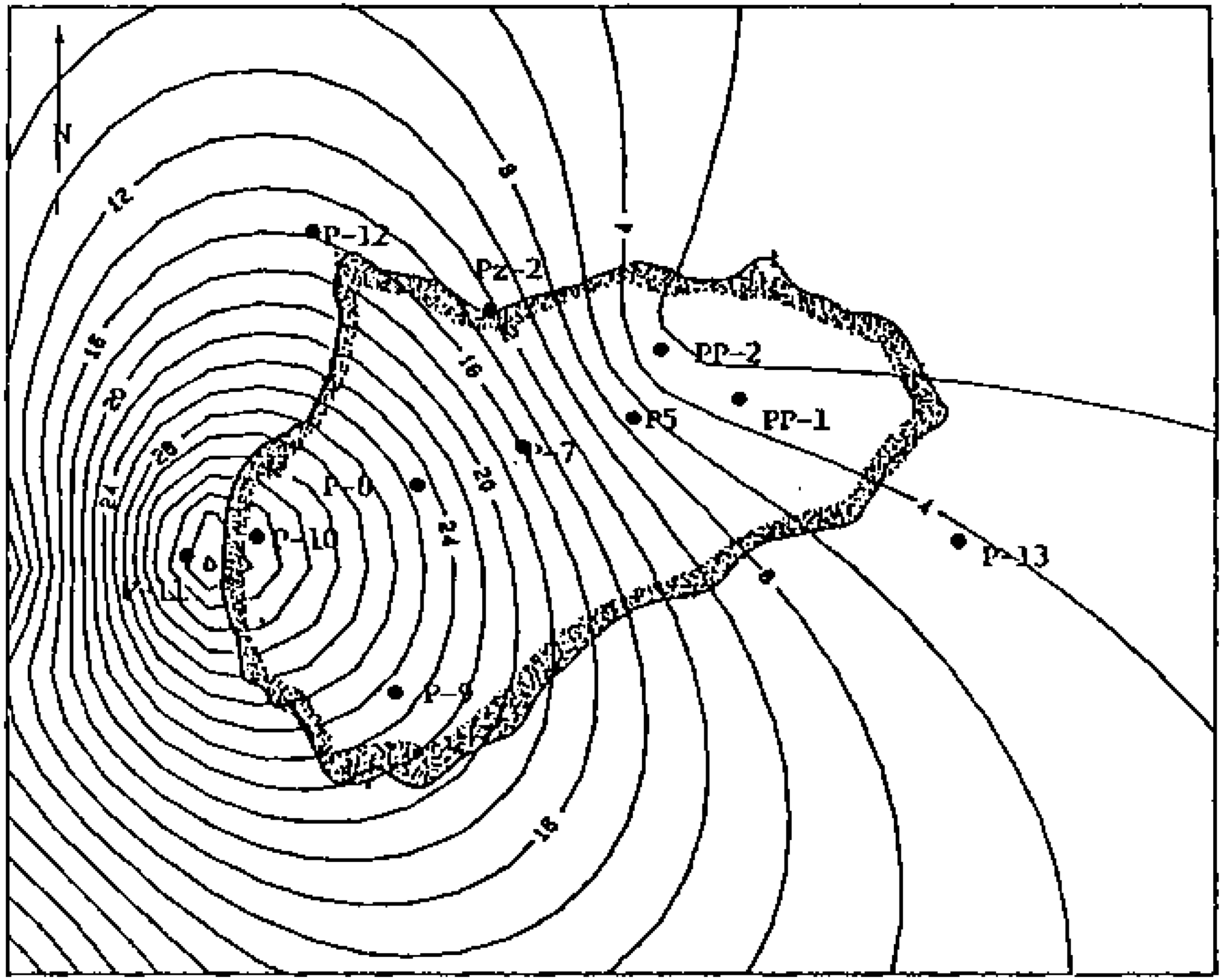

FIG. 5 SO_4 at level A.

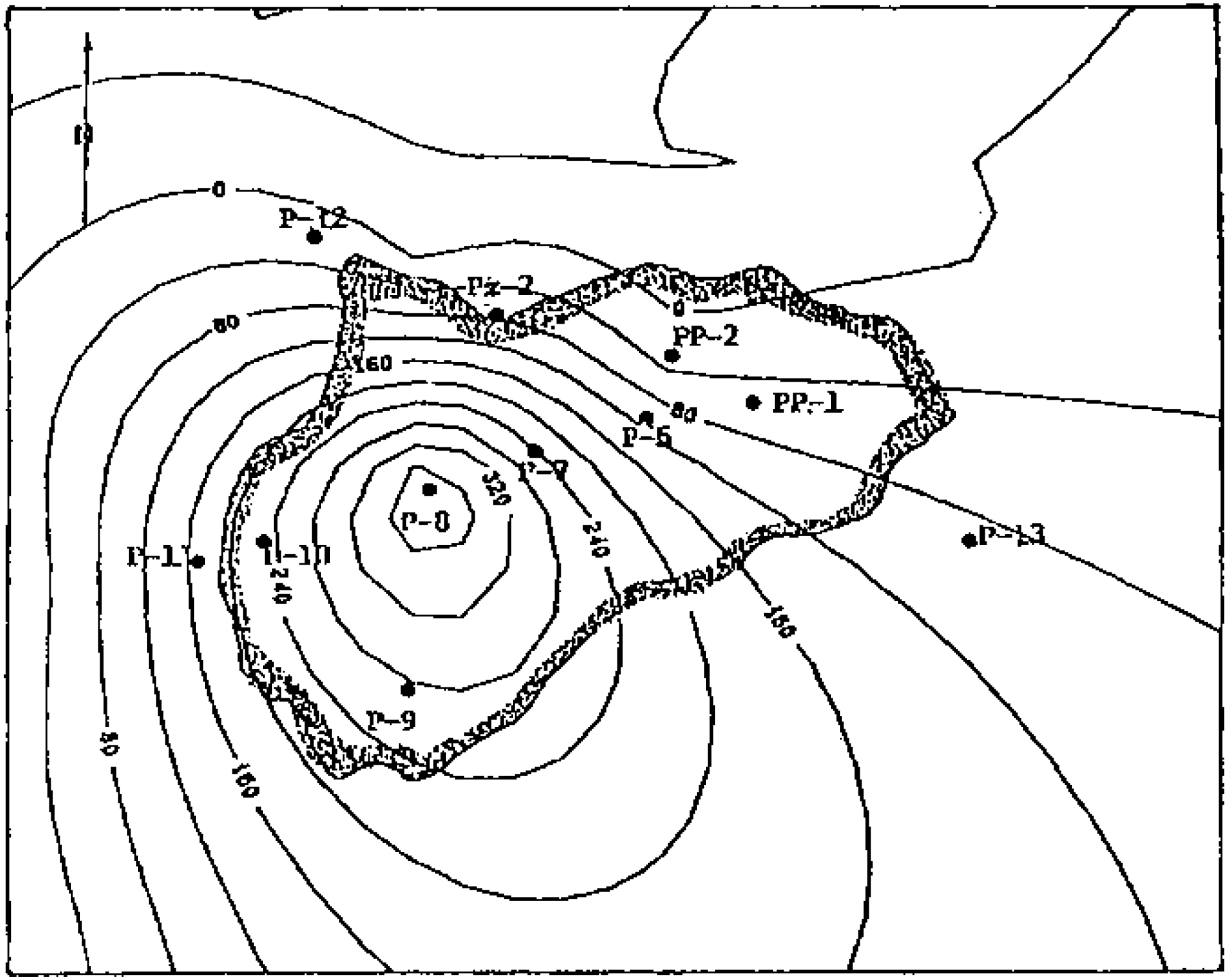

FIG. 6 PCB plume at level A.

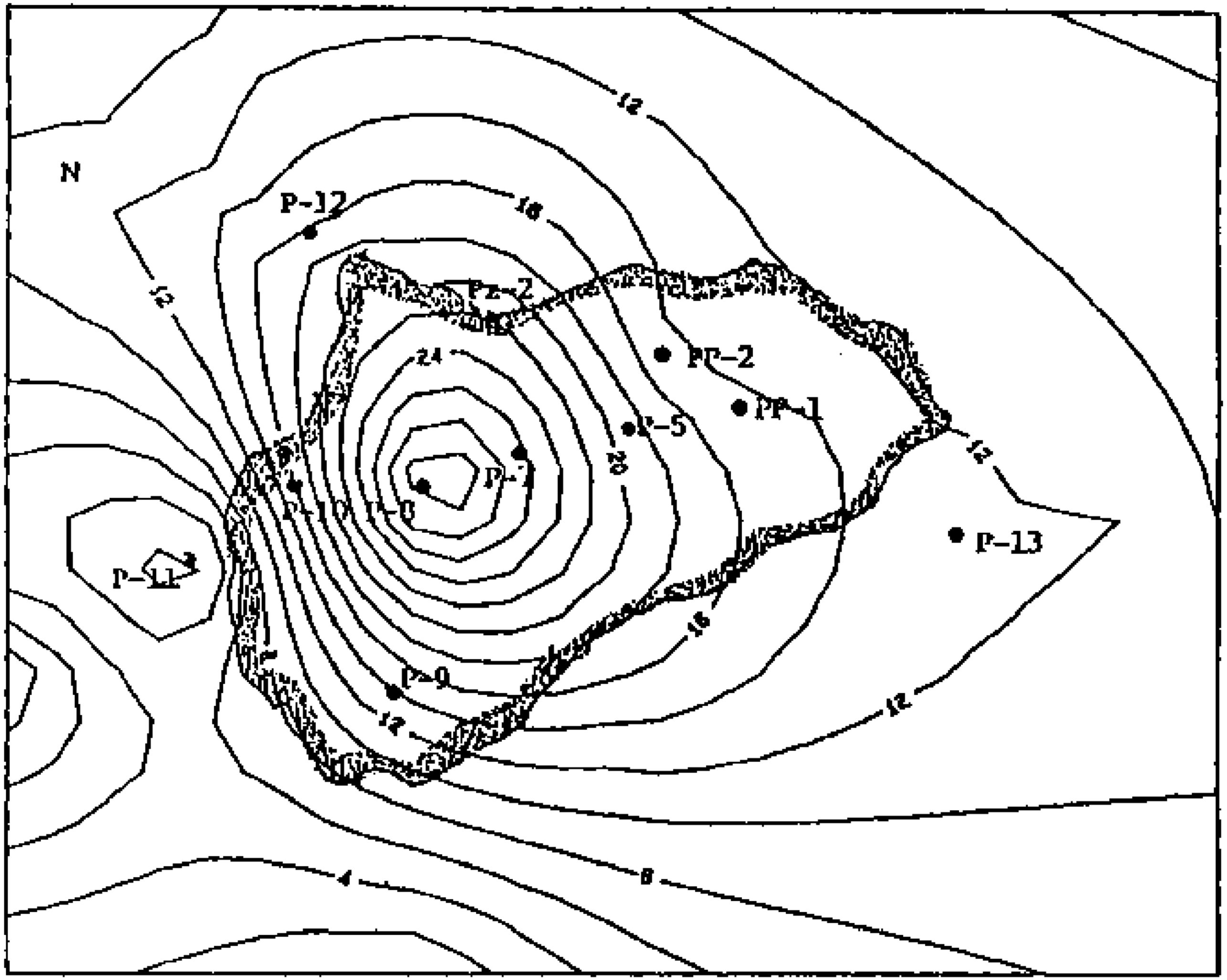

FIG. 7 Phenol at level A.